

VAGUS NERVE STIMULATION IN HYPERTENSIVE RATS: ASSESSING
PATHOPHYSIOLOGY USING ECG AND PRESSURE DATA

A THESIS
SUBMITTED TO THE FACULTY OF
UNIVERSITY OF MINNESOTA
BY

JAMES JONATHON SCHULTZ

IN PARTIAL FULFILLMENT OF THE REQUIREMENTS
FOR THE DEGREE OF
MASTER OF SCIENCE

ALENA TALKACHOVA

MAY 2017

© James Schultz 2017

Acknowledgements

I would like to sincerely thank my advisor, Dr. Alena Talkachova for allowing me to start a project in the lab before I was officially accepted as a Master's student, for guiding me throughout the research process, and for providing advice on various career paths I have been considering post-graduation. I would also like to thank Elizabeth Annoni, for putting up with my never-ending questions and providing extensive input on MATLAB code and rough drafts. I am grateful to my fellow lab members Kanchan Kulkarni, Steven Lee, Vasanth Ravikumar, Ryan Kluck, and Dr. Sharon Zlochiver, for providing much-needed critical commentary on thesis rough drafts and practice presentations. Thank you to Dr. Tay Netoff, Dr. Emad Ebbini, and Dr. Bruce KenKnight, for volunteering their valuable time to serve on my defense committee. Furthermore, I would like to acknowledge Rachel Jorgenson, the graduate program coordinator in the biomedical engineering department for always promptly and informatively answering my many logistical questions. Lastly, I would like to thank my family for their continued support and encouragement during my academic endeavors.

Abstract

Hypertension, which is associated with an imbalanced autonomic nervous system, is becoming an increasing problem in the US and worldwide, and new therapies are needed, since not all patients respond to current medications. Vagus nerve stimulation (VNS), which aims to restore autonomic balance, has emerged as a promising new treatment for this disease. In our lab, we conducted an experimental study aimed at assessing the safety and efficacy of chronic, continuously cyclic VNS to attenuate the development of hypertension in spontaneously hypertensive rats. Hypertension was induced via a high salt diet and rats were randomized into two groups: Sham Control (n=6) and VNS Treatment (n=6). In vivo blood pressure and electrocardiogram (ECG) were monitored continuously by an implantable telemetry system. We developed and validated methods to calculate time and frequency domain metrics for heart rate variability and blood pressure variability. Additionally, the sequence method in the time domain was employed to measure baroreflex sensitivity. Artifacts and ectopic beats can cause errors in the analysis of these metrics, so we also developed and validated robust pre-processing methods to edit ECG and pressure data in order to acquire clean signals. Results show that hypertension leads to decreased heart rate variability, decreased baroreflex sensitivity, and increased blood pressure variability, all of which are indicative of pathophysiological effects of hypertension. VNS may preserve heart rate variability blood pressure variability and baroreflex sensitivity at certain frequencies.

Table of Contents

List of Acronyms	iv
Chapter 1: Introduction	1
Overview of Hypertension	1
Physiology Review.....	2
Assessing ANS Through Cardiovascular Variability	7
Vagus Nerve Stimulation.....	12
Goals of the Thesis	13
Chapter 2: Methods	15
Experimental Protocol.....	15
Data “Pre-Processing”	16
Data “Post Processing”	25
Frequency Domain Methods	26
Statistical Analysis.....	32
Chapter 3: Results	33
Survival Data.....	33
Mean Heart Rate and Blood Pressure	34
Heart Rate Variability and Blood Pressure Variability	34
Baroreflex Sensitivity	41
Chapter 4: Discussion	43
Survival Data.....	43
Average BP and HR.....	43
Frequency Domain Parameters – Unresolved Questions	44
Effects of Hypertension on Sham Rats	46
VNS Rats: Effects of Stimulation	48
Baroreflex Sensitivity	49
Limitations	51
Future Work and Recommendations.....	52
Chapter 5: Conclusion	53
References	55
Appendix A: Physiological Correlates of Cardiovascular Oscillations	59
Appendix B: Instructions for MATLAB	65

List of Acronyms

ANS	Autonomic Nervous System
ASDNN	Average of the Standard Deviations of NN Intervals
BRS	Baroreflex Sensitivity
BP	Blood Pressure
BPV	Blood Pressure Variability
CO	Cardiac Output
CVP	Central Venous Pressure
DBD	Day Before Death
DBP	Systolic Blood Pressure
ECG	Electrocardiogram
HF	High Frequency
HR	Heart Rate
HRV	Heart Rate Variability
HTN	Hypertension
LF	Low Frequency
MAP	Mean Arterial Pressure
PI	Pulse Interval
PSD	Power Spectral Density
PNS	Parasympathetic Nervous System
RAAS	Renin-Angiotensin-Aldosterone System
RMSSD	Root Mean Square of Successive Differences
SBP	Systolic Blood Pressure
SDANN	Standard Deviation of the Averages of NN Intervals
SDNN	Standard Deviation of NN Intervals
SNS	Sympathetic Nervous System
SV	Stroke Volume
TPR	Total Peripheral Resistance
ULF	Ultra Low Frequency
VLF	Very Low Frequency
VNS	Vagus Nerve Stimulation
W6	Week 6
W9	Week 9

CHAPTER 1: INTRODUCTION

Overview of Hypertension

Hypertension, or abnormally elevated arterial blood pressure, can be classified as either primary or secondary. Primary, or essential hypertension is high arterial blood pressure that has no identifiable root cause (idiopathic), and it is this type that afflicts 95% of patients diagnosed with hypertension [1]. Secondary hypertension refers to high arterial blood pressure with a clearly identifiable cause such as kidney disease or hyperthyroidism. This paper is concerned with primary hypertension, and any future mention of hypertension is referring to this type.

Primary hypertension afflicts 75 million Americans and almost 1 billion people worldwide, and greatly increases the risk for heart disease and stroke, the first and third leading causes of death in the US, respectively [1], [2]. Current guideline-directed treatments call for a regimen of antihypertensive medications along with dietary and lifestyle changes; however, not all patients comply and/or respond to these treatments [3],[4]. Treatment resistant hypertension, defined as peripheral arterial blood pressure that remains elevated despite concurrent use of three antihypertensive agents of different classes, is becoming more prevalent and an increasing problem. It is estimated that 20-30% of all “hypertensives” have the treatment resistant type [5]. There is a clear unmet need for new and effective alternative treatments for these patients who do not respond to drugs, hence the recent focus on device-based approaches, such as VNS.

Despite decades of basic and clinical research, primary hypertension still has no firmly established etiology, although some of its pathophysiology has been identified. Strong evidence has shown that hypertension is associated with autonomic imbalance characterized by sympathetic hyperactivation and parasympathetic withdrawal [6]–[8]. Vagus nerve stimulation, which aims to rebalance the autonomic nervous system, has emerged as a promising solution to combat the autonomic imbalance associated with the hypertensive state.

Physiology Review

Control of Blood Pressure

To understand how an imbalanced autonomic nervous system (ANS) plays a role in hypertension (HTN), it is important to review how blood pressure (BP) physiology and control mechanisms operate under normal conditions. At any moment, the pressure gradient across the vasculature is equal to the central venous pressure (CVP) subtracted from the mean arterial pressure (MAP). This gradient is equal to the product of cardiac output (CO) and total peripheral resistance (TPR). Since CVP is at or near 0 mmHg, the equation becomes:

$$\text{MAP} = \text{CO} \times \text{TPR} \quad (1.1)$$

TPR refers to the resistance to blood flow realized by all the systemic vasculature. This resistance is usually dependent on vessel diameter, but can also be affected by blood viscosity and vessel length. CO is a volumetric flow rate and represents the volume per

time pumped by the heart, usually expressed in L/min. Since CO is equal to the product of stroke volume (SV) and heart rate (HR), equation 1.1 can be rewritten:

$$\text{MAP} = \text{SV} \times \text{HR} \times \text{TPR} \quad (1.2)$$

Each of the three variables on the right of this equation is influenced by complex physiological parameters and the variables may also interact with one another. The overall system is summarized in Figure 1.1. The ANS, made up of the sympathetic nervous system (SNS) and parasympathetic nervous system (PNS), can modify virtually all the variables in Figure 1.1, either directly via post-synaptic effects of neurotransmitters, or indirectly by activating hormonal systems. For example, acute increases in SNS activity will affect the heart and vasculature almost immediately, resulting in increased CO and TPR, and thus BP. The SNS also acts on a longer time scale, to promote renin release in the kidney, which increases sodium and water retention and raises blood volume [9]. In summary, increased SNS activity tends to promote higher BP, both acutely and chronically, and PNS activity promotes the reverse.

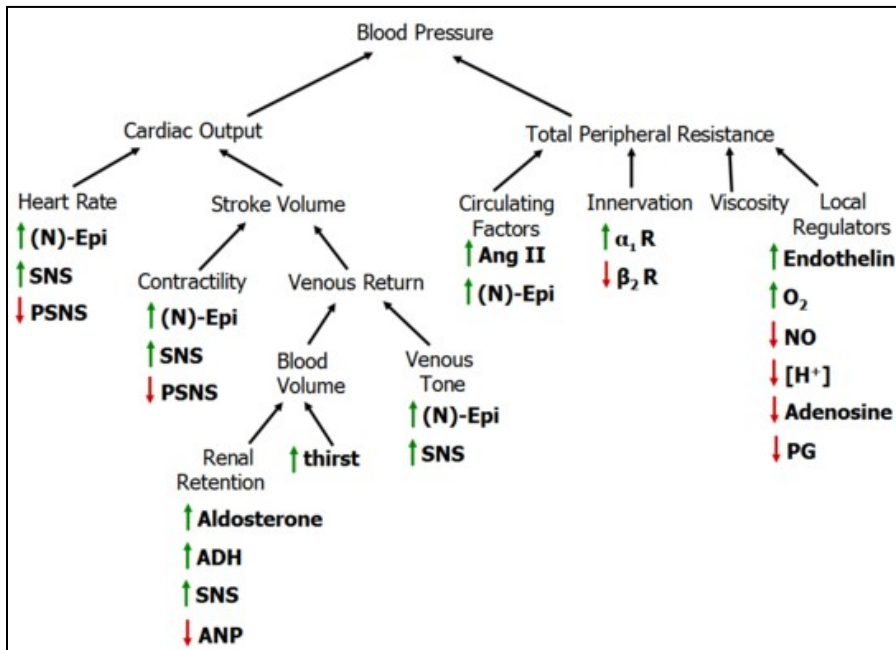


Figure 1.1: Factors that influence blood pressure (Reproduced with permission from [9]).

Negative Feedback Systems in Blood Pressure

Many different systems “sense” BP perturbations that deviate from a set point and react in a way that tends to return BP to that same set point. This phenomenon is often referred to as BP homeostasis. One of the most prominent negative feedback loops involved in BP homeostasis is the baroreflex. Arterial baroreceptors located in the aorta and carotid sinuses increase their firing rate in response to stretching of vessel walls. An increase in MAP leads to an increased firing rate of the receptors, and a decrease in MAP leads to a decreased firing rate. These receptors then transduce and relay this pressure information, in the form of afferently propagating action potentials, to the medullary brain stem where it is processed and neural responses are activated [1]. This afferent

portion of the baroreflex is displayed on the left side of Figure 1.2, and the efferent portion of the baroreflex is displayed on the right side.

The efferent portion consists of the sympathetic branch and the parasympathetic branch. The sympathetic branch innervates the sinoatrial (SA) node and atrioventricular (AV) node in a way that increases HR as well as conduction velocity. Sympathetic nerves can also significantly alter contractility (force production) of the heart and innervate blood vessels, leading to increased TPR. All of these changes work together to raise BP (see equation 1.2). The parasympathetic branch of the baroreflex consists of the right and left vagus nerves. These nerves innervate the heart at the SA and AV nodes to reduce HR and conduction velocity. Parasympathetic nerves also sparsely innervate the periphery of the heart, so can slightly reduce contractility. Vagal efferents do not predominantly innervate the vasculature so do not modify TPR [9]. The baroreflex acts by adjusting both the PNS and SNS simultaneously. If afferent discharge from baroreceptors is increased, signaling an increase in BP, the medullary control center will trigger a reflex response that activates parasympathetic efferent activity and inhibits sympathetic efferent activity, ultimately leading to a decrease in BP. The reverse will occur if afferent discharge decreases. Note that this efferent system does not solely belong to the baroreflex – other inputs are involved such as the chemoreceptor reflex; essentially, it represents the most direct and immediate method by which the ANS controls the cardiovascular system [1], [10].

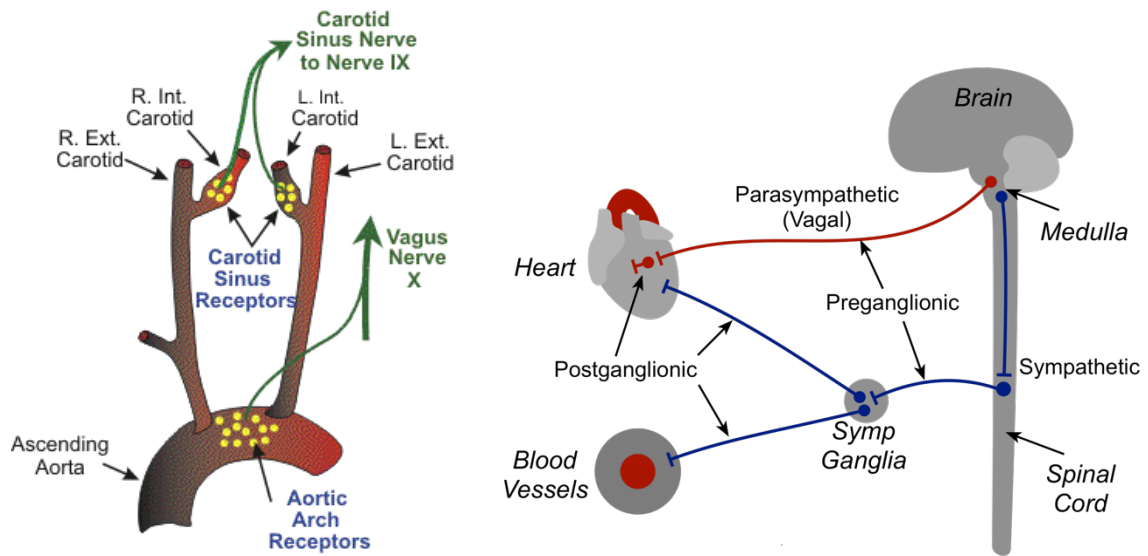


Figure 1.2: Baroreflex Arc. Left side displays receptors and afferent portion, right side displays efferent portion. Reproduced with permission from [1].

There are important time delay differences between the SNS and PNS responses in this efferent system. It has been shown that vagal efferent nerves are able to respond to pressure changes almost immediately and can affect HR on a beat-to-beat basis, whereas the SNS is characterized by a time delay and longer lasting effects [10], [11]. Therefore, the PNS has control of HR at higher frequencies, the implications of which will be discussed in subsequent sections. One biochemical explanation for the differing delay times for PNS and SNS effects on HR is that the SNS requires the use of the second messenger cAMP system to change heart dynamics whereas the PNS does not [12].

The baroreceptor reflex is considered “neural” control of BP, as is the chemoreceptor reflex, which has a similar negative feedback loop. Humoral control of HR and BP through circulating hormones also occurs and has been shown to be slower-

acting than neural control [10], [11]. Humoral factors which affect BP include circulating catecholamines, the renin-angiotensin-aldosterone system (RAAS), atrial natriuretic peptide, anti-diuretic hormone (vasopressin), and others [1]. Local mechanisms, such as the myogenic vascular response and the endothelial nitric oxide system are able to regulate BP on a local level by altering vessel caliber, and can operate independently of neurohormonal influences [9]. The control of BP involves many different control loops operating with different time constants. It's important to note that many of the control loops are interdependent and constantly interacting. For example, an activation of the baroreflex may cause autonomic innervation of the heart through vagal or sympathetic efferent nerves, generating a fast response, but this same activation may also play a role in longer-term hormonal control mechanisms.

Assessing ANS Through Cardiovascular Variability

Overview

In daily life, external perturbations initiate BP fluctuations, and neural and hormonal control mechanisms respond to oppose these perturbations to bring BP back to a reference “set point.” Therefore, rather than being random noise, variability in HR and BP can reflect the health and performance of cardiovascular homeostatic mechanisms. Almost all of the mechanisms to control BP discussed in the previous section are affected by cardiovascular diseases, including HTN. [13].

Heart rate variability (HRV), or variation in the time between heartbeats, has become a popular clinical and investigational tool over the past 30 years [14]. In HRV

analysis, it is generally the changes in RR-interval that are analyzed rather than changes in HR. The RR interval is constantly changing on a beat-to-beat basis, but also varies over larger time intervals from hours to days. It has been shown repeatedly that the ANS plays a significant role in the production and modulation of these oscillations, and that HR measures can give insight into the underlying pathophysiology of the ANS under many different maladies; additionally, certain HRV measures offer significant prognostic value [8], [15]–[18]. Reduced HRV has been linked to increased mortality in both humans and animals and has been shown to be prevalent in hypertensive patients [6], [19].

Blood pressure variability (BPV) is less established as a marker of autonomic function, but is closely linked to HRV, and the simultaneous analysis of HRV, BPV and the baroreflex that links BP to HR may provide deeper insights into underlying pathophysiology. Compared to HRV, BPV has less standardized methods for measurement, although studies typically define BPV as variation occurring in the sequences of systolic, diastolic, or mean arterial pressures calculated at discrete time points. BPV does not refer to differences between systolic and diastolic pressures, which is termed pulse pressure. In the case of VNS, it makes sense to measure oscillations in both HR and BP, since the ANS regulates many of these oscillations, and VNS has been shown to directly affect the ANS [20].

Measurement Techniques

There are many established methods for measuring HRV (and less so BPV), which can be categorized into two main groups: time domain techniques and frequency domain techniques. In frequency domain analysis, either fast Fourier transformation or auto-regression techniques are used to decompose the signal into its frequency components. Historically, fluctuations in RR interval and BP have been categorized into four different “types,” or frequency bands: high frequency (HF), low frequency (LF), very low frequency (VLF) and ultra low frequency (ULF) oscillations. Frequency domain parameters are calculated as the area under the curve of the power spectral density (PSD) in the frequency range of interest. These frequency ranges can differ between studies, but common values for humans are displayed in Table 1.1. A representative power spectrum of a 24-hour recording of RR intervals in a human displaying the four frequency bands is shown in Figure 1.3. Researchers have attempted to correlate each of these frequency bands in Figure 1.3 to various physiological mechanisms; a detailed discussion of these correlations is presented in Appendix A.

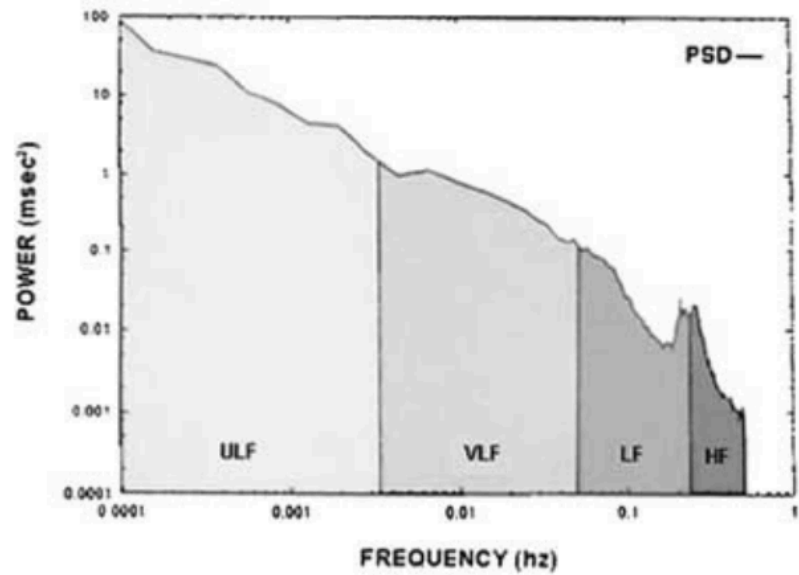


Figure 1.3: Power spectral density showing frequency bins. Reproduced from [21]

Table 1.1: Frequency bands as defined in humans from [21]

Frequency Band	Frequency in Humans	Period of Oscillation in Humans
High Frequency (HF)	0.15-.4 Hz	2.5 - 6 seconds
Low Frequency (LF)	0.04-0.15 Hz	6-25 seconds
Very Low Frequency (VLF)	0.0033 -0.04 Hz	25 seconds to 5 minutes
Ultra Low Frequency (ULF)	Less than 0.0033 Hz	Greater than 5 minutes

In time domain analysis, intervals between adjacent “normal” QRS complexes are calculated to acquire a recording of NN (Normal-to-Normal) intervals (as opposed to RR-intervals, which retain intervals due to ectopic beats) [14]. Note that noise and arrhythmic episodes can greatly influence HRV measurements and need to be removed carefully (editing of data is discussed in the methods section).

SDNN is the standard deviation of all NN-intervals over a certain time period; usually a 5 minute or 24 hour recording is used, although other time lengths are permitted and have been used in studies [17]. However, if different time lengths are used, caution must be taken in making any cross-study comparisons. SDANN is the standard deviation of the average of NN intervals. To calculate SDANN, compute the average NN interval over a 5-minute segment, and then take the standard deviation of these averages. Essentially, it is akin to applying a moving average filter to the NN intervals and then taking a standard deviation.

$$\text{SDANN} = \text{std}(\mu_1, \mu_2, \dots \mu_N) \quad (1.3)$$

SDANN effectively “filters” out oscillations with periods shorter than 5 minutes. This metric is less subject to editing errors than SDNN because the averaging over 5 minutes minimizes effects due to unedited artifacts, missed beats, and arrhythmias [21]. ASDNN is the average of the 5-minute standard deviations of NN intervals. ASDNN is calculated by taking the standard deviation of 5-minute NN interval segments, and then averaging these standard deviations. ASDNN reflects oscillations with periods less than 5 minutes in length; it removes long-term effects such as those due to circadian rhythms and hormonal systems.

$$\text{ASDNN} = \text{mean}(\text{std}_1, \text{std}_2 \dots \text{std}_N) \quad (1.4)$$

RMSSD is the root mean square of successive differences. This calculation consists of calculating successive differences between NN intervals, squaring each

difference, adding these squared differences together, and then taking the square root of the sum. It is meant to gauge the amplitude of high frequency oscillations.

$$\text{RMSSD} = \text{sqrt}(\text{mean}(\Delta D_1^2, \Delta D_2^2 \dots \Delta D_n^2)) \quad (1.5)$$

A visual representation of these time domain parameters based on data acquired in this study is presented in the results section, “Qualitative Examination of Data.”

Vagus Nerve Stimulation

In theory, there are two ways to combat the imbalanced ANS associated with HTN. “Beta-blockers” have long been established as a treatment for HTN with the goal of reducing the functional effects (adrenergic receptor activation) of sympathetic activity; however, this treatment does not directly impact diminished cardiac vagal tone that accompanies autonomic imbalance [22]. VNS is original in its ability to augment vagal tone.

The mechanisms underlying the effects of chronic VNS are not fully understood. Acutely, stimulation of the efferent fibers of the vagus nerve bundle may cause chronotropic (reduced HR), dromotropic (reduced AV conduction velocity), and inotropic (reduced contractility) effects on the heart; however, these acute effects are probably not the primary cause of long term benefits of VNS [20], [23]. Kakinuma et al showed that efferent VNS was able to produce cardioprotective effects via acetylcholine release in the heart independent of HR-decreasing effects [24].

Ostensibly, chronic VNS results in long-term vagal up-regulation on a broad level, and therefore improved autonomic balance [23]. This vagal up-regulation may

result in a concomitant reduction in sympathetic activity, owing to the two systems' antagonistic effects on each other [22]. For example, electrical stimulation of the cardiac parasympathetic nerves is reported to attenuate norepinephrine (a SNS neurotransmitter) spillover in the left ventricle [25]. Zhang et al showed that VNS reduced plasma angiotensin II levels in dogs with heart failure, and Mancina et al demonstrated that activation of vagal efferents can decrease the release of renin [23], [26]. Mancina's study provides further evidence that VNS reduces SNS activity, but also indicates that VNS therapeutic effects may partially result from an inhibited RAAS. Lastly, VNS has anti-inflammatory and antioxidant effects. Zhang et al also showed in their study of VNS-treated dogs that plasma-C reactive protein, a marker of inflammation, was significantly reduced. In summary, VNS has been shown to have complex and diverse therapeutic effects that may manifest through many different pathways.

Goals of the Thesis

Vagus nerve stimulation has emerged as a promising new treatment for essential HTN and it is the goal of our lab to evaluate its efficacy in treating HTN and HTN-induced heart disease. This thesis aims to contribute to this overall goal through the analysis of ECG and pressure data derived from HTN and VNS-treated HTN rats. Early on in the research, we discovered a clear need in our lab for new approaches to evaluate autonomic and physiological function using solely ECG and pressure data. Therefore, a primary goal is to investigate and implement in MATLAB recent approaches that use ECG and pressure data to assess cardiovascular health. While other metrics were

investigated, this thesis will exclusively focus on HRV, BPV and baroreflex sensitivity. We also discovered that extensive pre-processing of data is required in order to accurately calculate HRV, BPV, and baroreflex sensitivity; these metrics are easily corrupted by artifacts of both physiological and technical origin. Thus, another product of this thesis is a development of pre-processing methods in MATLAB aimed at acquiring clean data sets, Lastly, the completed MATLAB software will be applied to data extracted from both hypertensive rats with VNS treatment and rats without treatment, to better elucidate underlying physiological effects of vagus nerve stimulation.

CHAPTER 2: METHODS

Experimental Protocol

Dahl Salt Sensitive (DS) male rats (29-35 days old, Charles River Laboratories, Wilmington, MA) were used in this study. These rats offer a genetic model of HTN that develops early and is maintained by a high salt diet [27]. After 4 weeks of 8% NaCl high salt diet (S100001, Research Diets, Inc., NJ, USA), vagus nerve stimulators (Demipulse, Model 103, Cyberonics, Inc, Houston, TX USA) and telemetry systems (HD-S11 Data Sciences International, St Paul, MN USA) were implanted, and rats were randomly divided into two groups: HTN-VNS (n = 6, with functional VNS stimulator implants), and HTN-Sham (n = 6, with nonfunctional VNS stimulator implants of the same mass). Bipolar cuff platinum-iridium electrodes were placed around the right cervical vagus nerve and common carotid artery bundle, and the pulse generator (8 cc, 14 g) was implanted subcutaneously and positioned in a subcutaneous pocket on the back of each rat. Parameters of the intermittent VNS are displayed in Figure 2.1 along with a timeline of the study. These parameters were determined based on previous studies performed in the lab by Elizabeth Annoni. A pressure-sensing catheter was implanted into the descending aorta via the left femoral artery, and two ECG leads were fixed subdermally onto the chest muscle. Electrograms and arterial pressure were recorded at 500 Hz. Rats were conscious and freely moving in their home cages for the duration of the in vivo portion of the study.

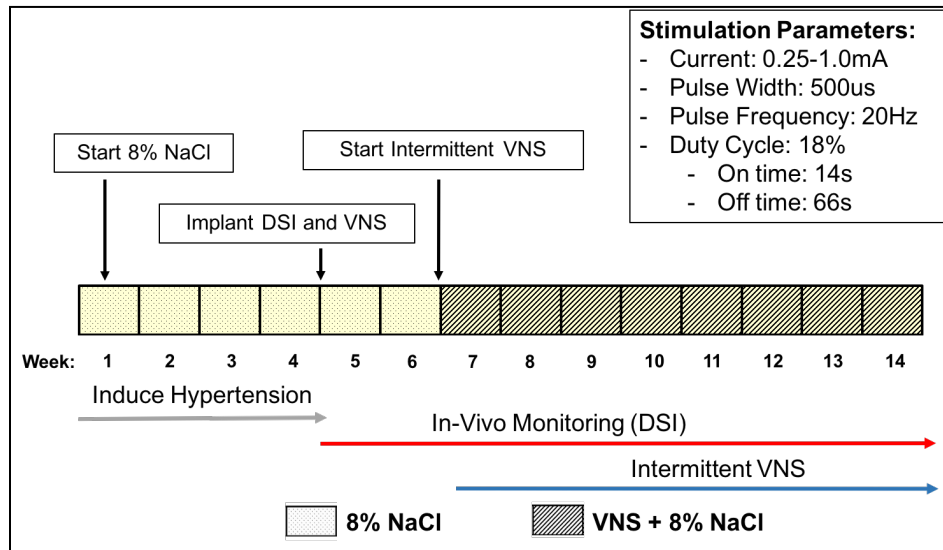


Figure 2.1: Timeline of experiment.

Data “Pre-Processing”

After rat death, we analyzed approximately 12 hours of raw ECG and BP data as follows: 4 hours from week 6 (W6), 4 hours from week 9 (W9), and 4 hours from day before death (DBD). Some rats did not live until W9, so W9 was omitted for these rats (see Figure 3.1). The four-hour segments were taken from 10:00 PM- 2:00 AM, during “wake time” when rats are most active, and sympathetic activity is highest. To enable a more robust analysis, we extracted data from Ponemah software as ASCII (American Standard Code for Information Interchange) files, then converted and uploaded them into MATLAB. In previous studies, most analysis had been completed in Ponemah or other commercial software so the use of MATLAB to quantify HRV, BPV and baroreflex sensitivity was a novel technique used in our lab, with all code written de novo. After the data was uploaded to MATLAB, several filters were applied to remove noisy segments.

Peltola gives a detailed explanation on the editing of RR interval data in [28], and the procedures used in this study are in line with instructions presented there. We adapted other editing and analysis procedures from the Task Force of the European Society of Cardiology’s recommendations on HRV, as well as Bernston et al [10], [17]. In addition, we reviewed and incorporated techniques used in rat studies in which HRV and BPV analysis was performed [11], [29]–[33].

The first filter removed saturated signals of pressure and ECG, meaning extreme high-valued, “non-physiological” noise. The filter then spliced together the segments on either side of the removed saturated portions as seen in Figure 2.2.

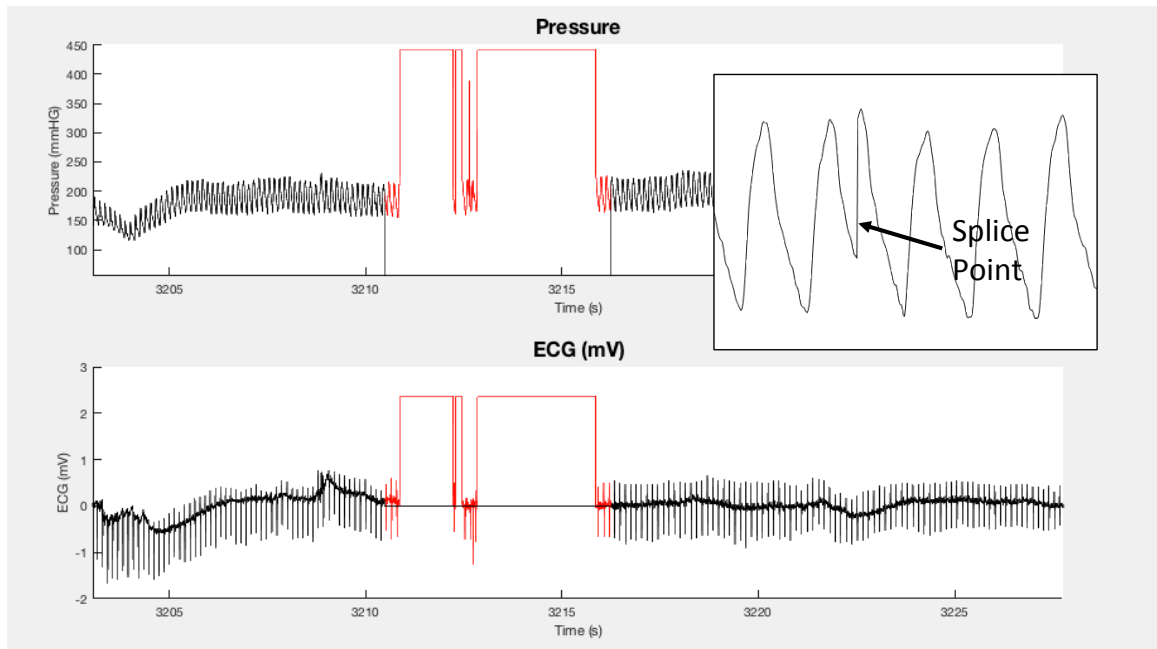


Figure 2.2: Removal of saturated segments of data, with an example of a splice point displayed.

Splicing introduces a point in the data that can lead to incorrect calculation of RR intervals, so minimizing the number of splices is ideal. To minimize splice points, when

two saturated segments existed in close proximity to each other, the filter algorithm removed both saturated segments, as well as any “clean” data in between the two segments. Therefore, some clean data was sacrificed. The splice points that remain were dealt with through subsequent editing techniques. For some data traces, removal of saturation resulted in a shortening of the data set as demonstrated in Figure 2.3. The shortest data set after saturation removal was 168 minutes, and to ensure uniformity of length, all other data sets were cut to 168 minutes.

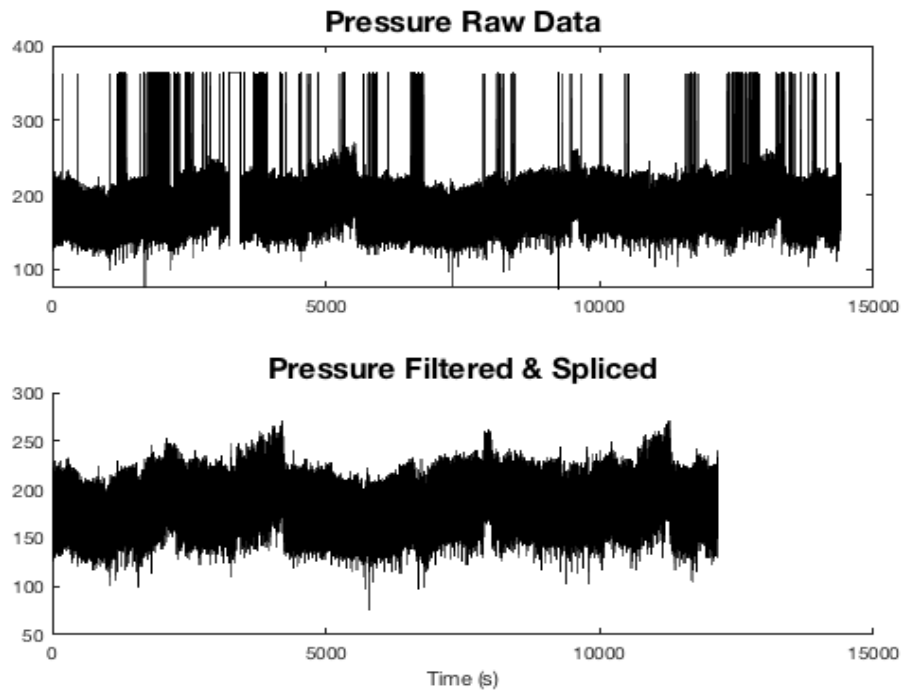


Figure 2.3: In this data file, removal of saturation points resulted in a significant shortening of the data trace.

After the initial filtering to remove saturation, systolic blood pressures (SBP), diastolic blood pressures (DBP) and QRS complexes were calculated using a peak-finding function in MATLAB. RR intervals were initially calculated as the time

difference between two consecutive QRS complexes. To identify the QRS complex, established methods such as the Pan-Tompkins algorithms and others were first used, but these proved unsatisfactory (many QRS Complexes were not identified accurately during stimulation and with other artifact effects) [34]. We therefore created a custom algorithm that identified the QRS complex based on peak size, and temporal proximity to the nearest systolic and diastolic peaks in the pressure trace (Figure 2.4). In this way, each QRS complex must have an associated systolic peak and diastolic peak. This algorithm proved accurate and was validated under a variety of conditions, including during stimulation and during ectopic beats. If examined closely, it can be seen in Figure 2.5 that the QRS peak is calculated correctly during stimulation, as depicted as the lighter colored triangles.

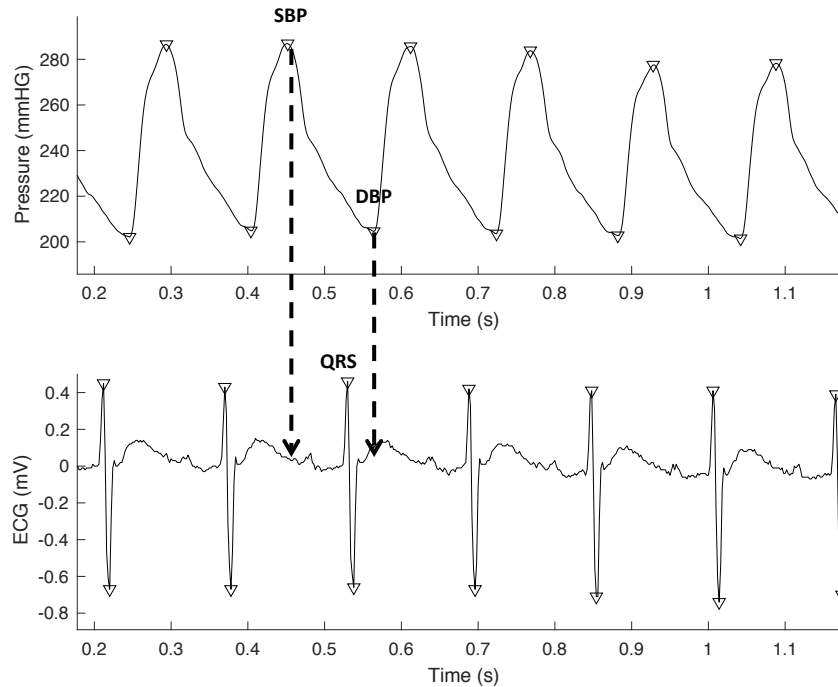


Figure 2.4: Algorithm for detecting QRS complex based on temporal proximity to previous SBP peak and subsequent DBP peak.

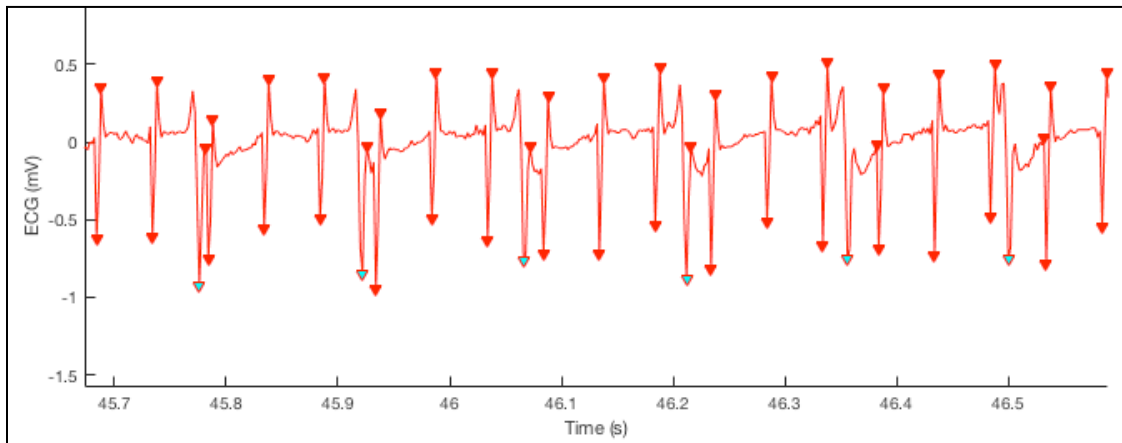


Figure 2.5. The algorithm detected correct QRS complexes (seen as the lighter colored triangles) during vagus nerve stimulation periods.

While this algorithm seemed to work well, it was abandoned after it was discovered that two of the rats had ECG traces in which QRS complexes were entirely indiscernible, even visually (Figure 2.6).

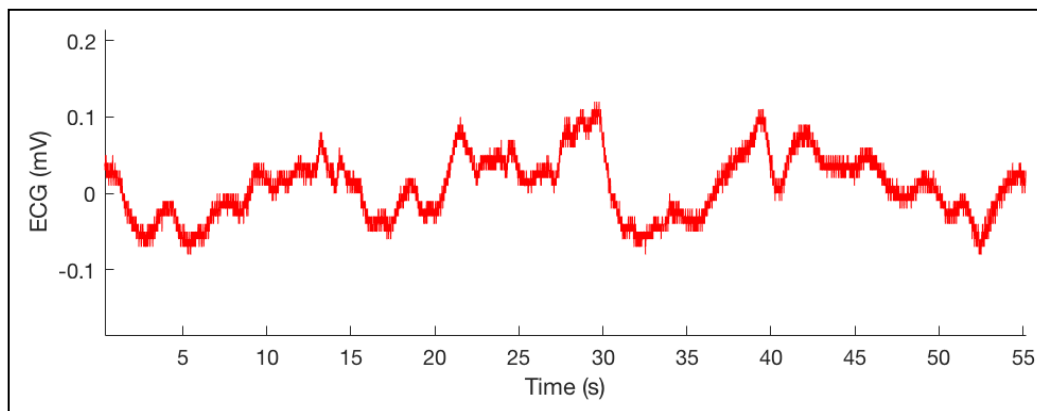


Figure 2.6. Some ECG traces had indiscernable QRS complexes.

We therefore decided that HR information would have to be gleaned from the BP trace. Pulse interval (PI), the time difference between two consecutive systolic (or diastolic) peaks, was first used to replace RR interval calculated from ECG data. For

most of the data, this method worked well, but under certain situations led to incorrect calculations; for some of the data, there was a relatively wide range in which a systolic peak could be defined. Figure 2.7 displays how this phenomenon can lead to “short” and “long” PI’s being calculated. This small error in calculation appears as noise in the pulse interval trace (Figure 2.8). Therefore, we took the derivative of the pressure and calculated peaks from this data trace in order to calculate pulse interval (PI), as seen in Figure 2.7. This method proved more accurate and corresponded well to RR interval (Figure 2.8).

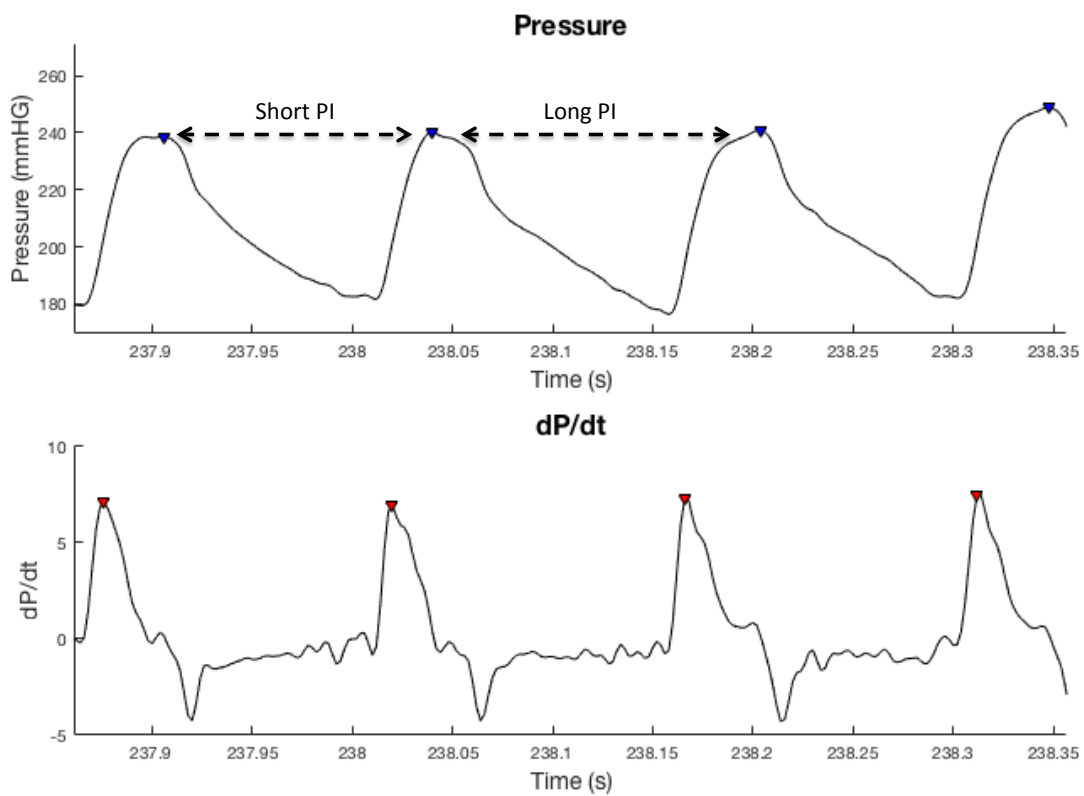


Figure 2.7. Some pressure traces had a wide systolic peak, which could lead to shorter or longer PI's being calculated in certain cases.

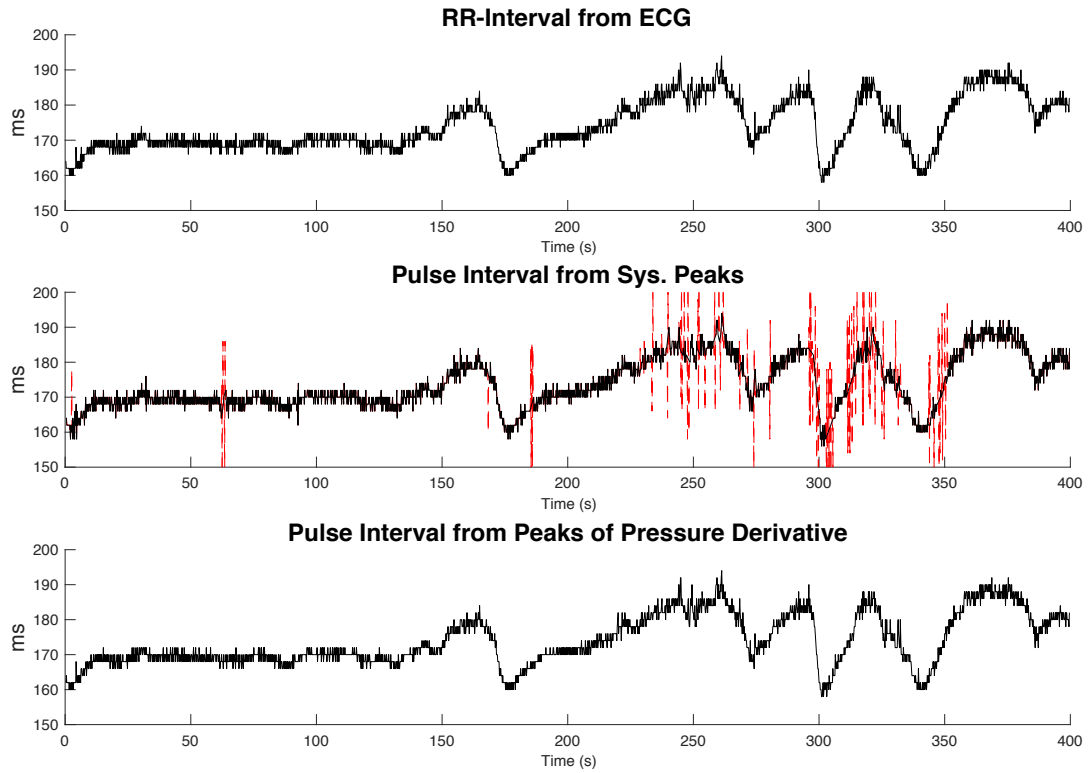


Figure 2.8. Methods for calculating intervbeat interval. In the second subplot, calculating pulse interval from systolic peaks leads to errors in calculation which cause noise. This noise is shaded a different color because originally it was removed with a filter.

Since PI is used, both BP data and HR data are derived from the pressure trace, and the ECG trace becomes irrelevant. After systolic peaks were calculated, an algorithm was employed to “match” every systolic peak with its subsequent derivative peak (the peak calculated on the pressure derivative trace). This matching algorithm is necessary to ensure a 1:1 correspondence between systolic peak and derivative peak, and thus pulse interval. This matching is mainly important for baroreflex sensitivity analysis, but is also an initial filter for arrhythmic events in which 2 systolic peaks occur in a row with only 1

corresponding RR interval. The matching protocol is depicted in Figure 2.9: SBP_i is matched with PI_{i+1} , giving a delay of 1: this information is important for baroreflex sensitivity analysis, which is discussed in a later section.

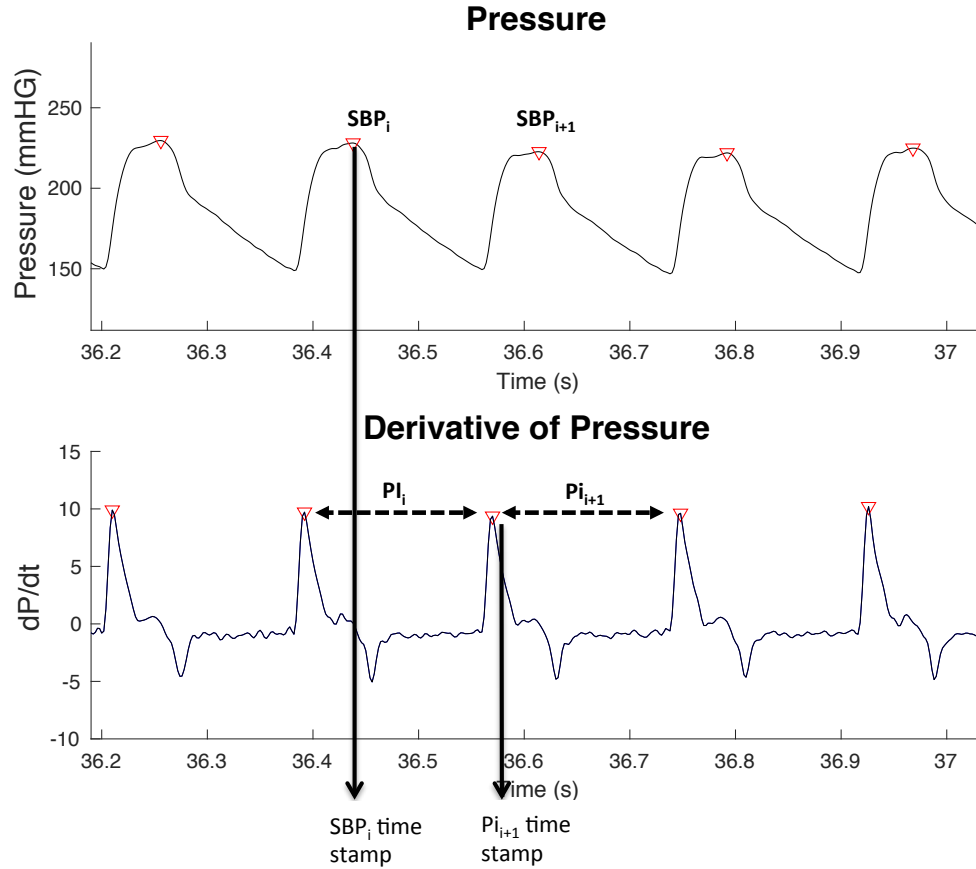


Figure 2.9: Matching protocol between SBP and PI ensures a 1:1 correspondence. Time vectors were recorded to store the timings SBP and PI samples. The time of SBP_i is straightforward; it's recorded as the time at which the peak occurs. The “time stamp” for PI is taken as the time of the first peak used in the calculation.

After SBP and PI signals were acquired and “matched,” they had to be put through additional filters to remove arrhythmias and remaining non-physiological noise, which can significantly influence BPV and HRV calculations [28]. In addition, the

“splice” points discussed earlier led to the calculation of incorrect systolic peaks in some cases. These next filtering steps required several iterations. In Aubert et al, two filters were used for rat RR interval data: a percentage filter, that removes any value that deflects by more than 20% of previous one and replaces this value by the mean value of the five preceding and five following values, and a second filter that removes and replaces deflections that differ by more than three standard deviations from the overall mean value. Both of these filters were experimented with, but proved unsatisfactory for data sets in this experiment – they tended to unnecessarily remove data that was not due to ectopic beats. Instead, a filter similar to the “percentage filter” was used; if a value differed by more than $\pm 'X'$ mmHg, it was removed and replaced via linear interpolation. Interpolation, rather than deletion, is the recommended method of several sources [10], [28]. The value ‘X’ was arrived at by visually examining the data set and choosing the value of X that appears to best remove ectopic artifacts; if it is too high, than data is unnecessarily edited, if it is too low, than artifacts can remain. Thus, the value ‘X’ was “customized” for each rat data set. ‘X’ was initially set at 20 mmHg and this value worked well for the majority of data sets, but for a few of them, had to be lowered to ensure all artifacts were removed. While this visual customization method may seem crude, there is a basis for it in the literature. In “Role of Editing,” Peltola explains: “many experts believe that manual editing with visual verification of the R-R intervals and a careful choice of the appropriate editing method is a more reliable method and can never be fully replaced by the current automatic correction systems.” Thus, filtering methods

used here were in line with HRV expert's current recommendations. Results of the filter described above are displayed in Figure 2.10.

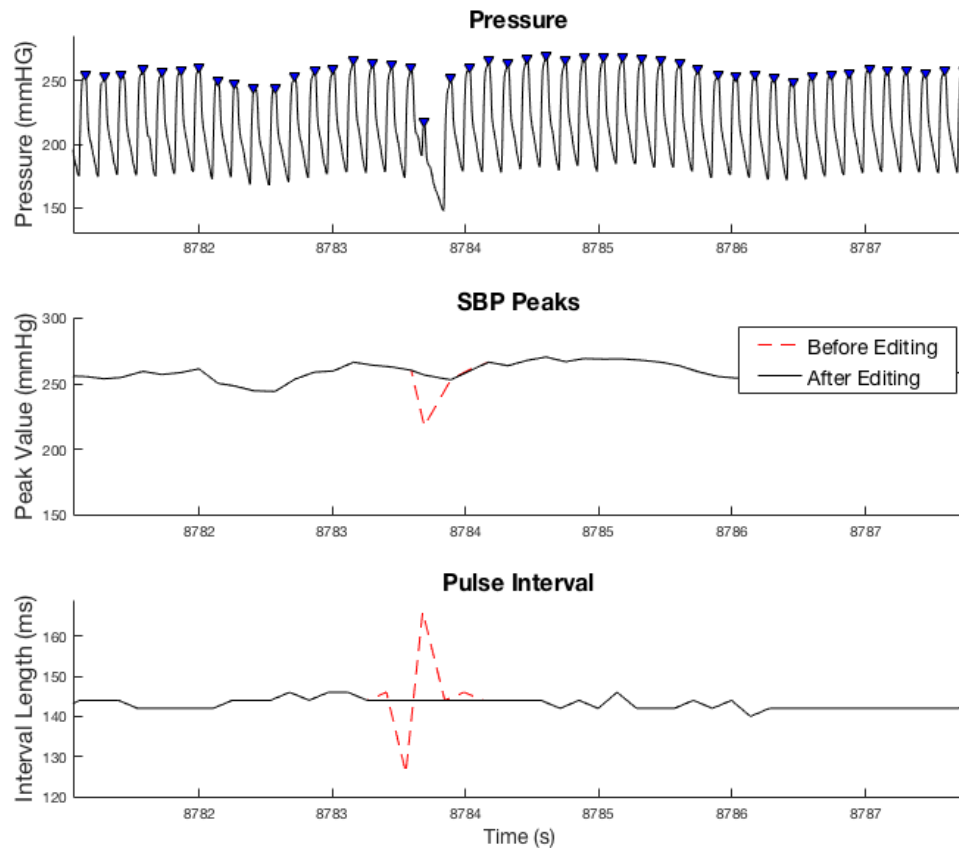


Figure 2.10: Removal of ectopic beats and replacement via linear interpolation.

Data “Post Processing”

Once the SBP and PI signals are calculated with noise removed, data “post processing” can take place, in which time and frequency domain parameters for HRV and BPV are calculated, as well as baroreflex sensitivity (BRS) using the sequence method. MATLAB code was created to calculate the time domain parameters discussed in the introduction: SDNN, SDANN, ASDNN, and RMSSD. Time domain calculations were

straightforward and are not elaborated upon. There are several different methods to calculate frequency domain parameters, which are described next.

Frequency Domain Methods

For frequency domain methods, the PI and SBP sequences first need to be resampled, since HR and SBP values occur at uneven sampling intervals. Following a technique described in Aubert et al, “Analysis of HRV in unrestrained rats: Validation of Method and Results, ” the signals were first de-trended and then resampled using spline interpolation at 10 Hz; this frequency was chosen as an adequate resampling frequency to ensure HR’s up to 600 beats per minute (BPM) could be captured without any loss (aliasing) of information (600 BPM is equivalent to a heart period of 100 ms). In this way, the discrete point processes are approximated by a continuous function sampled at 10 Hz.

The power spectral density was calculated using the fast Fourier transform (FFT) in MATLAB in two distinct ways. The first technique was fairly straightforward; the power spectrum was calculated for the entire 168-minute data set, and ULF, VLF, LF, and HF power were calculated as the area under the power spectrum in the corresponding frequency band (Figure 2.11). Authors have used several different ranges for the frequency bands in rats, which are displayed in Table 2.1.

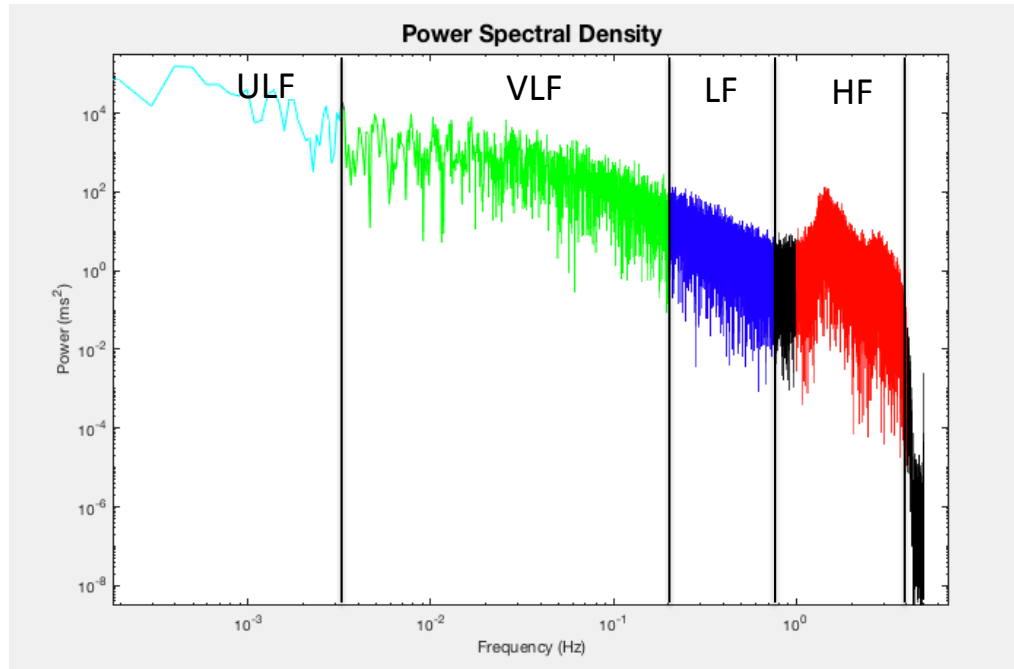


Figure 2.11. Power spectrum of entire data set in rats. The peak in the HF range at around 1.4 Hz corresponds to the respiratory rate in rats of 85 breaths/min [35]

Table 2.1: Frequency ranges used in rats

Parameter	Cerutti, Gustin et al	Cerutti, Barres, et al	Henze et al	Stauss	Aubert et al	Ning et al
HF Power Range (Hz)	0.75 – 3.85	0.76 – 5	1-3	1-4	0.78-2.5	0.78- 2.5
LF Power Range (Hz)	0.27 – 0.74	0.27 – 0.74	0.05-1	0.2 -0.6	0.19-.74	0.195- 0.74
VLF Power Range (Hz)	0.015-.255	0.0195 – 0.25	N/A	0.02- 0.2	N/A	N/A
ULF Power Range (Hz)	No study found in which ULF power was measured in rats.					

The second technique was performed according to a procedure used by Cerutti et al in their studies of rats, which aims to acquire more accurate calculations for HF and LF power [30], [31]. For each 168 minute recording, the data was divided into segments of 395 segments of $n=512$ points overlapping by one-half. For each segment, a PSD was calculated, and a corresponding HF and LF power were calculated (these data segments

were too short for VLF and ULF power). Outliers were then removed from the 395 values of HF and LF power and an average value was computed.

Several problems arose with frequency domain methods, which are presented in the discussion section. Based on these problems and some unanswered questions, we determined that further investigation is needed before frequency domain parameters, other than HF power, can be used to reliably gain information about the ANS for the data in our study. Therefore, only HF power computed using the second technique is the only frequency domain parameter presented in the results.

Baroreflex Sensitivity by the Sequence Method

As with HRV and BPV, both frequency domain and time domain methods exist for measuring the baroreflex. The “Sequence Method,” developed in 1985 by Berterini, is the most common one used in the time domain, and the parameter “measured” is termed Baroreflex Sensitivity (BRS) [36]. BRS can be measured in other ways than the sequence method, but BRS is usually defined as the change in inter-beat interval per unit change in BP [37]. In its early days, BRS was measured by triggering a change in BP by giving patients an intravascular injection of a vasoconstrictive or vasodilative agent and observing changes in HR [38]. In recent years, researchers have turned to measuring BRS noninvasively, by observing the “spontaneous baroreflex,” meaning sequences that occur due to fluctuations in BP that occur spontaneously throughout a normal day [38]. The sequence method involves identifying sequences of a minimum number of consecutive beats characterized by either a progressive rise in SBP and lengthening of PI, or a

progressive decrease in SBP and shortening of PI. Examples of baroreflex sequences are displayed in Figure 2.12. Each sequence has an associated regression line and gain (slope of regression line). BRS is calculated as the average value of the gains for all sequences.

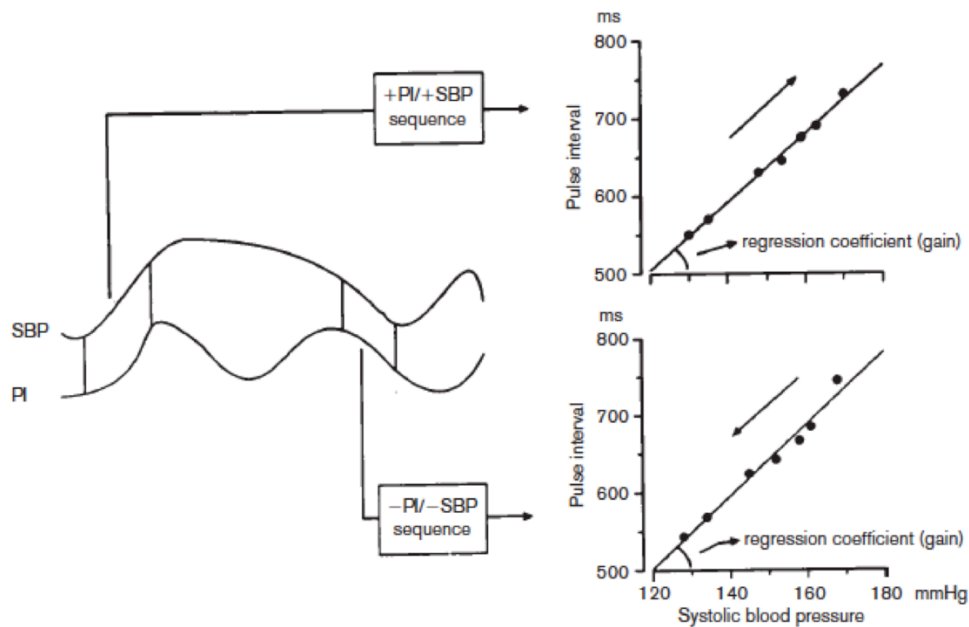


Figure 2.12: Baroreflex sequences from [38].

There are threshold criteria associated with the sequence method which are detailed in [37] and [38]. Most studies use a minimum coefficient of correlation (R^2 value), which refers to the linear fit of the regression line seen in Figure 2.12.

Additionally, a minimum number of points in a sequence are required; usually, three or four beats. Lastly, a minimum rise or drop in pressure and sometimes RR interval can be required. MATLAB code was developed to carry out the sequence method. As mentioned, systolic peaks were matched with subsequent pulse intervals calculated from derivative peaks with a delay of 1.

After initial analysis, it was determined that the breathing frequency had a significant effect on the types of sequences observed. In Figure 2.13 it can be seen that respiratory oscillations are superimposed over lower frequency movements and that coherency between SBP and PI likely occurs at more than one frequency. At around 850 ms, a large decrease in SBP and a corresponding decrease in PI occur, indicating that the baroreflex is acting at this lower frequency. However, the sequence method algorithm does not detect this event because it is not a *constant* decrease in both variables; instead the decrease is disrupted by respiratory oscillations. To ensure the capture of lower frequency sequences, both the SBP and PI signals were low pass filtered to remove respiratory oscillations. The resulting signal is represented by the dotted line in Figure 2.13. The same number of data points and sampling interval were retained in the filtered data.

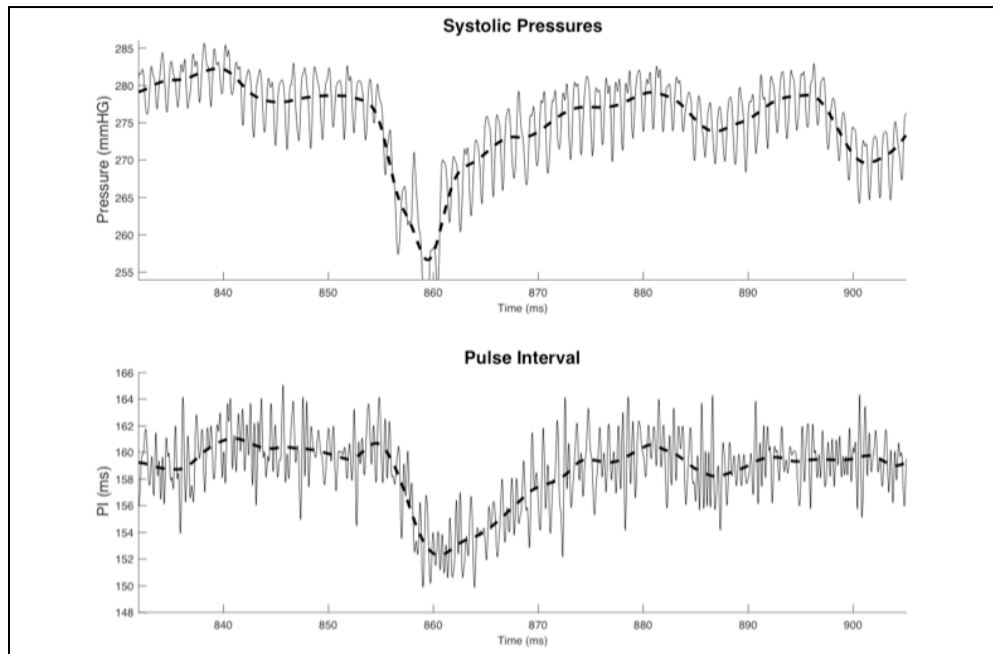


Figure 2.13: Dotted line represents low pass filtered data.

Figure 2.14 shows unfiltered SBP and PI samples and Figure 2.15 shows filtered SBP and PI signals, both after the application of the sequence method. The sequences depicted in Figure 2.14 are representative of coherence between SBP and PI at the respiratory frequency, while the sequences depicted in Figure 2.15 represent coherence over a lower frequency.

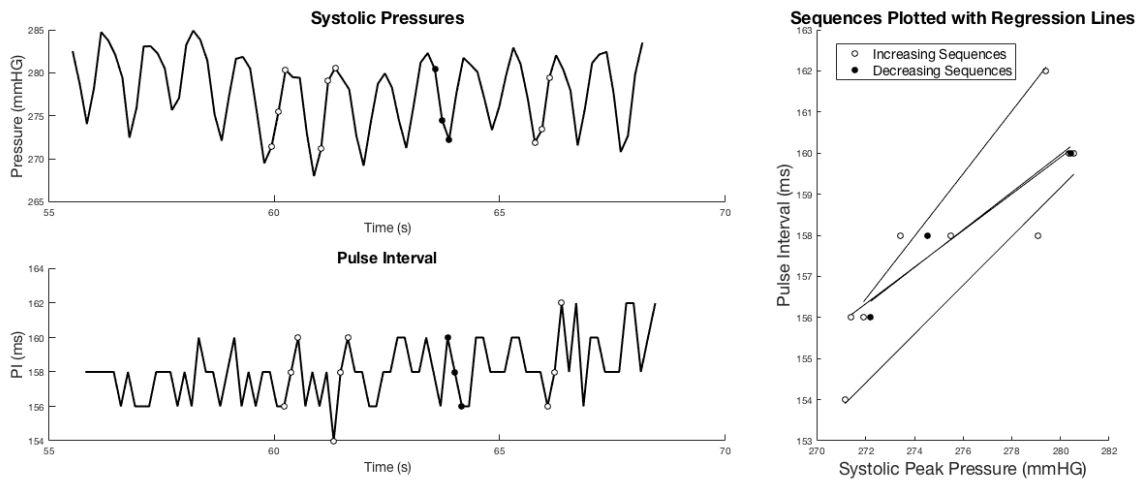


Figure 2.14: Sequence Method applied to unfiltered data

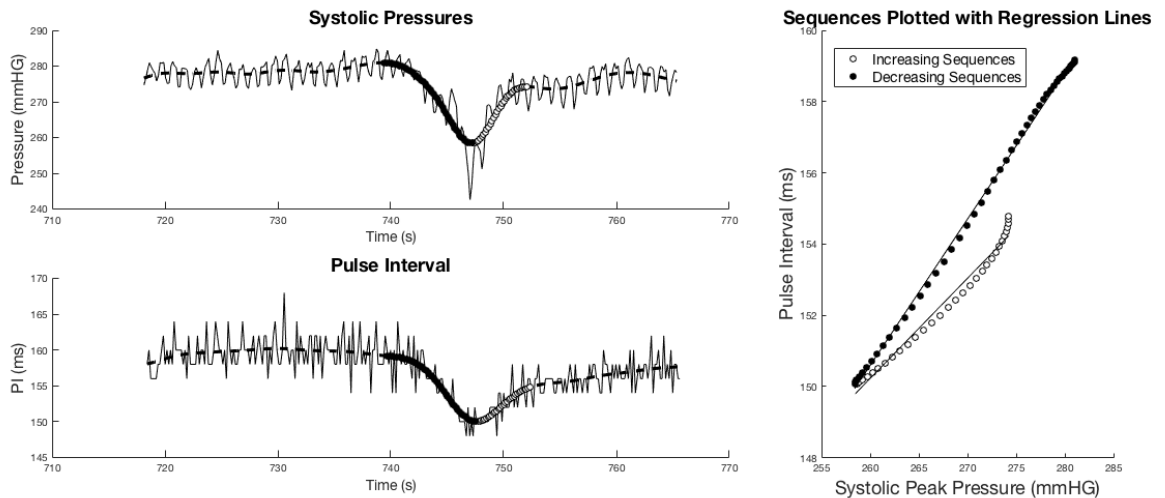


Figure 2.15: Sequence Method applied to filtered data.

Statistical Analysis

The paired t-Test carried out in Microsoft Excel was used to compare W6 results to DBD. In addition, W6 to W9 and W9 to DBD were also compared using the paired t-test. In addition, the changes in parameters from W6 to DBD were compared between Sham and VNS using a two-sample unequal variance t-Test. For example, Sham could have an average increase in a certain parameter, and VNS could have an average increase in the same parameter; it is these increases (or decreases) that are being compared.

CHAPTER 3: RESULTS

Survival Data

As a group, VNS Treatment rats survived longer than Sham Control rats after the start of VNS at W6 ($P < 0.05$). The average lifespan after W6 for Sham was 48% shorter: 20.2 days for Sham vs 38.8 days for VNS. Survival data for each rat is shown below. Note that only 3 Sham and 5 VNS rats were available for W9 analysis since some rats died before W9.

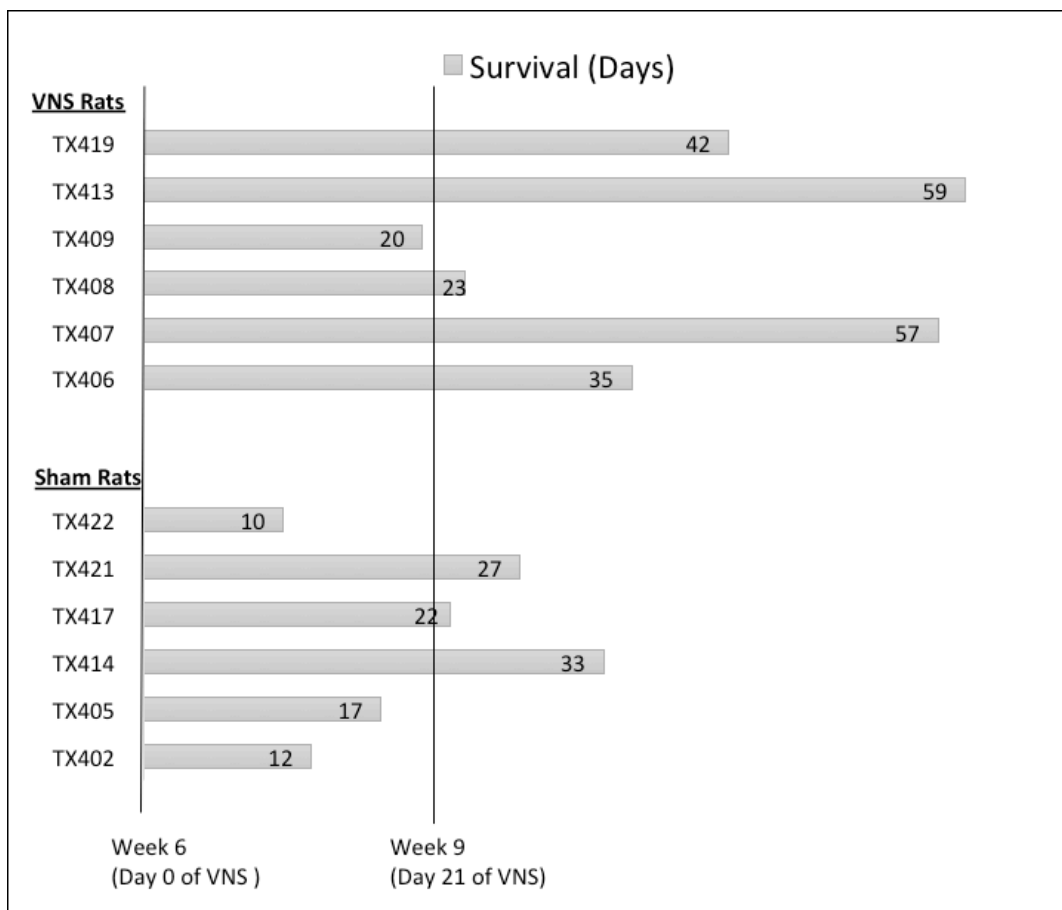


Figure 3.1: Survival Data - VNS outlived Sham.

Mean Heart Rate and Blood Pressure

Increases in SBP are seen in both Sham and VNS rats from W6 to DBD with statistical significance. No statistically significant trend is seen in mean HR for Sham nor VNS, although qualitatively mean prevailing HR appears to slightly decline in VNS rats over time.

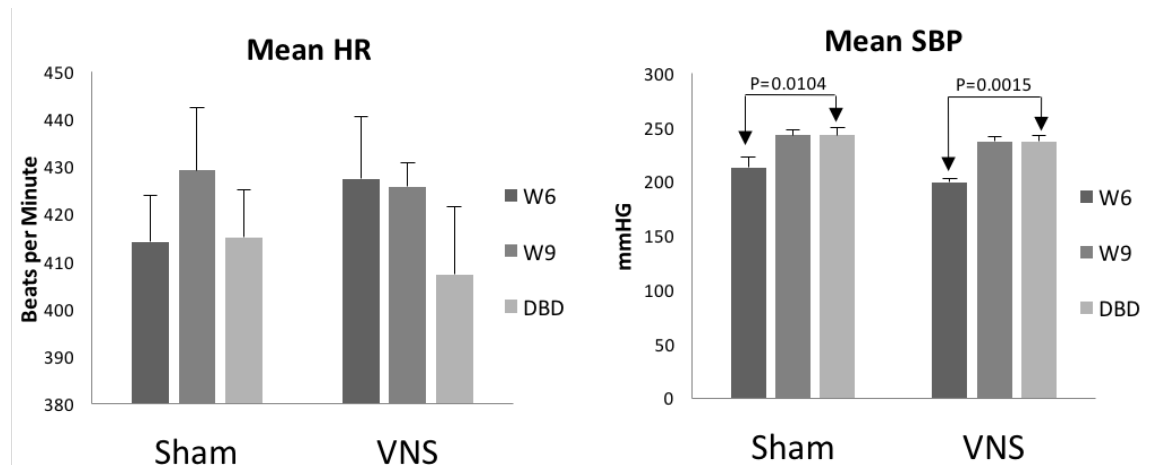


Figure 3.2: Mean HR and BP

Heart Rate Variability and Blood Pressure Variability

Methods were developed to measure HRV and BPV in both the time and frequency domain in MATLAB. However, later in the research, several issues arose with frequency domain methods that remain unresolved; these issues are presented in the discussion. Therefore, HF power is the only frequency domain parameter presented here.

Qualitative Examination of Data

Representative samples of data are shown in Figures 3.3 and 3.4 that provide visual aid in understanding time domain parameters.

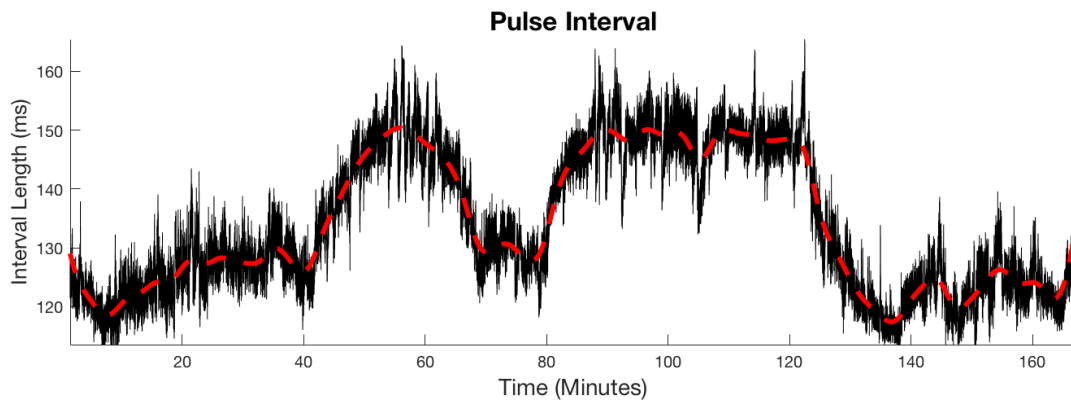


Figure 3.3: The dotted line above is the result of low pass filtering pulse interval at 0.0033 Hz

In Figure 3.3 above, a low pass filter with a cutoff frequency of 0.0033 Hz was applied to give the dotted line seen. Since SDANN averages every 5 minutes, it aims to track these long-term oscillations depicted by the dotted line: 1 divided by 300 seconds (or 5 minutes) is equal to 0.0033 Hz. ASDNN only measures oscillations with periods below 5 minutes: it quantifies oscillations that would remain if the dotted line were removed from the data above. SDNN quantifies oscillations across all frequencies, and is simply a standard deviation of the entire data set.

Figure 3.4 is a zoomed-in version of Figure 3.3. Respiratory oscillations are superimposed over lower frequency oscillations in this figure. RMSSD and HF power quantify these respiratory oscillations. HF Power was calculated using the 2nd technique presented in the methods. The frequency range for HF power was chosen as 1-4 Hz,

which is the value cited by Stauss [13]. The respiratory rate (as approximated by the location of the HF peak) of all rats in the study was above 1 Hz, so this range seems acceptable.

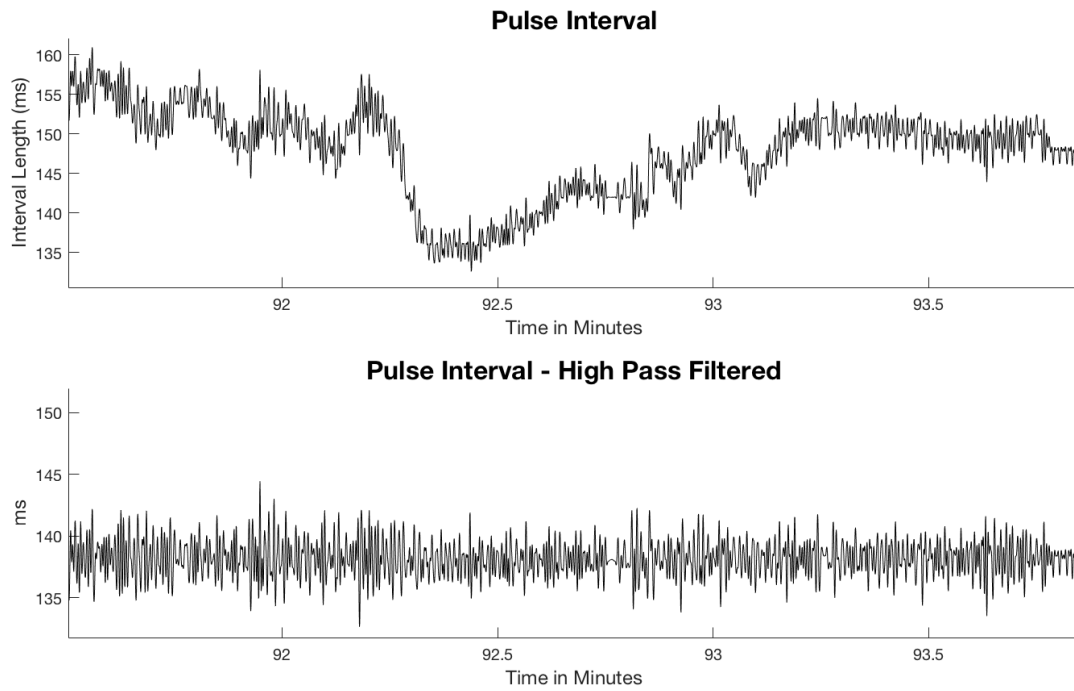


Figure 3.4: Only respiratory oscillations remain after high-pass filtering

Heart Rate Variability Plots

For HRV, SDNN, SDANN, and ASDNN all decreased for Sham rats, with statistical significance ($P < 0.05$) only seen in ASDNN (Figure 3.5). No statistical significance is observed for any of the parameters in VNS rats, although qualitatively VNS rats appear to decrease in HRV from W6 to W9, and possibly regain some of this variability (as measured by SDNN and SDANN) from W9 to DBD.

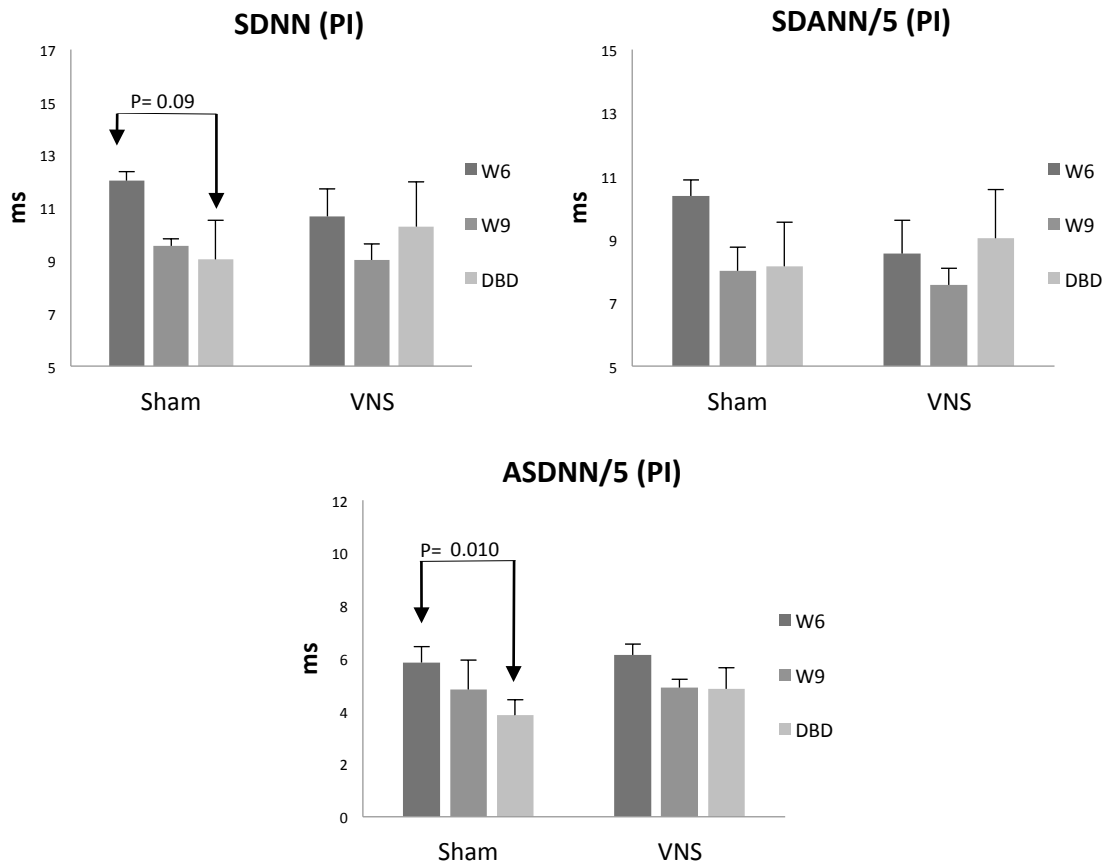


Figure 3.5: Time domain measures for overall HRV

HF power results appear to mirror results seen in RMSSD (Figure 3.6); this agrees with previous studies that have correlated RMSSD with HF power [21], and makes intuitive sense since both parameters are measuring high frequency respiratory oscillations. RMSSD and HF power from W6 to DBD decrease in Sham rats ($P=0.021$, $P=0.032$, respectively). Qualitatively these same parameters in VNS rats decrease slightly from W6 to W9, and from W9 to DBD appear to increase slightly; however, these trends don't attain statistical significance.

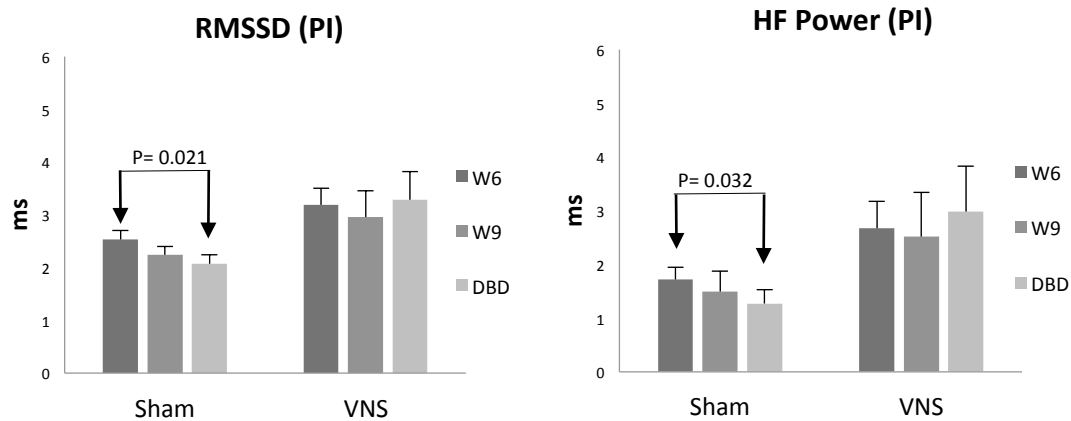


Figure 3.6: HRV at high frequencies

Blood Pressure Variability Plots

For BPV calculations, overall variability measured by SDNN increases from W6 to DBD in both Sham and VNS rats (no statistical significance). Both groups also increase in ASDNN (statistical significance was only seen for VNS rats, $P = 0.012$). SDANN appears to change very little from W6 to DBD.

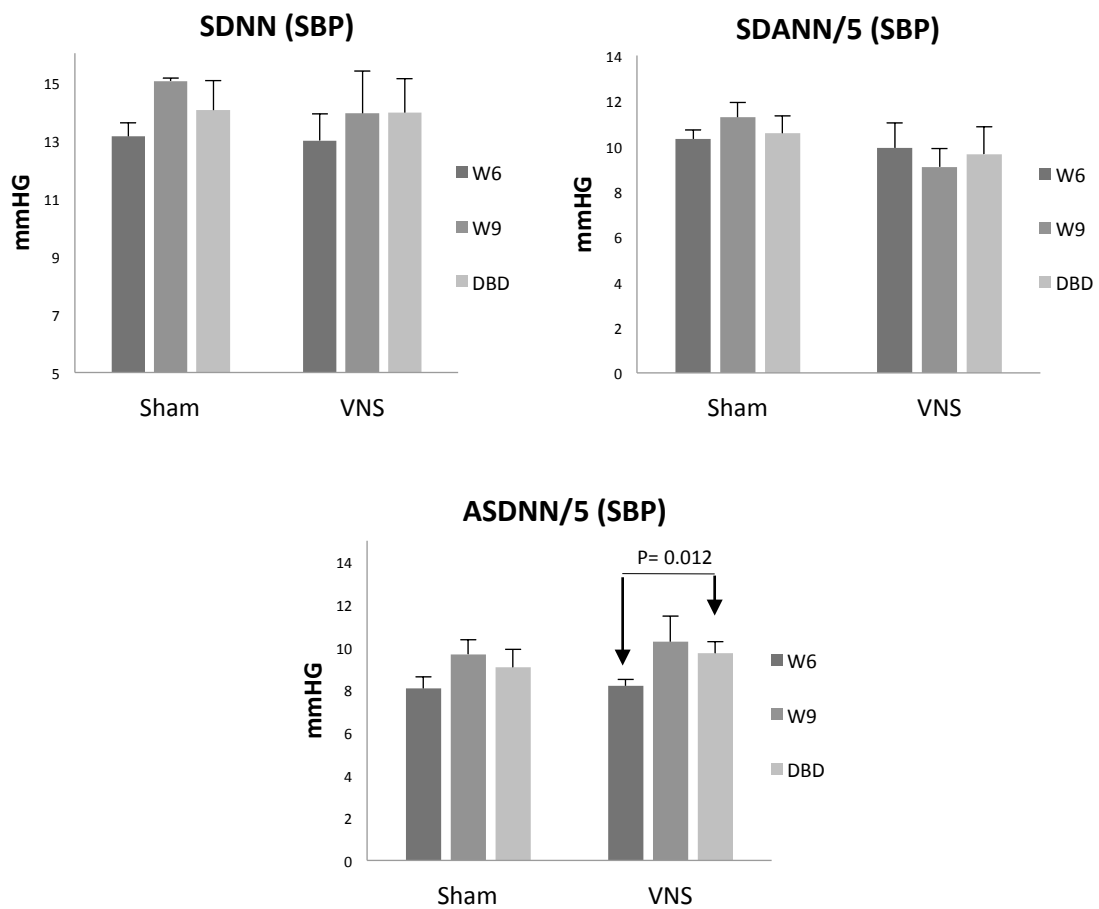


Figure 3.7: Time domain measures for overall BPV

Similar to HRV results, RMSSD and HF power mirrored each other for BPV.

Both parameters increased from W6 to DBD in both Sham and VNS rats, indicating that high frequency fluctuations in BP are increasing. High frequency fluctuations in BP are mechanically induced through respiration.

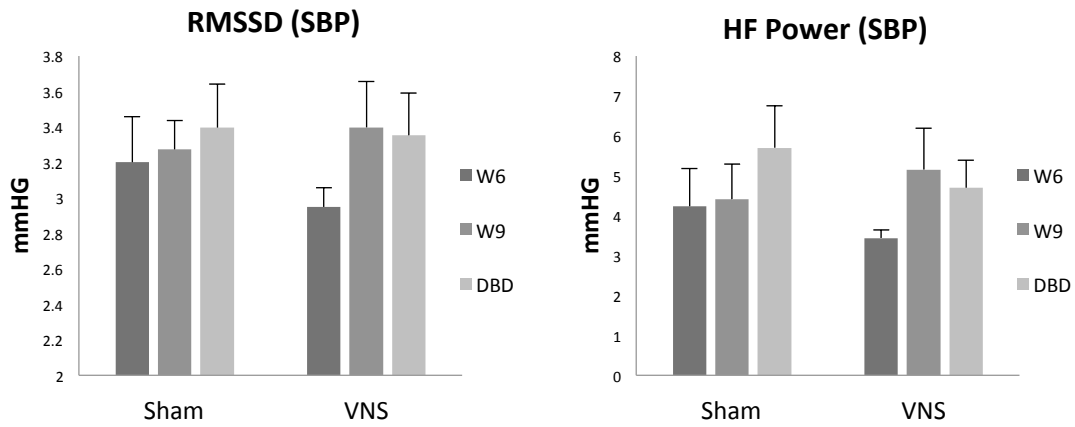


Figure 3.8: BPV at high frequencies

Baroreflex Sensitivity

Representative sequences obtained using the sequence method are displayed in the Methods section. As discussed there, the sequence method was applied to both raw data as well as filtered data in which the respiratory oscillations were removed. For the raw data, the following threshold criteria were used: minimum sequence count of 4, minimum required increase/decrease in pressure of 1 mmHg, and a minimum R^2 value of 0.9. These values are fairly standard and agree with values cited in the “EuroBaVar” study by Laude et al, which compares various methods for calculating baroreflex sensitivity [39].

The sequence method was also applied to filtered data. The filtering of data prior to application of the sequence method is a new technique, and no threshold criteria for this method have been established. Therefore, threshold criteria were manually tuned. If the minimum sequence count or required pressure change were too low, the algorithm would pick up sequences that did not look like baroreflex sequences. Therefore, threshold criteria were raised from the values used for unfiltered (raw) data in order to be more restrictive. This alteration of threshold criteria occurred based on a visual examination of which threshold values appeared to accurately capture baroreflex sequences. The following parameters worked well: minimum sequence count of 16, a minimum required increase/decrease in pressure of 5 mmHg, and a minimum R^2 value of 0.9. Other threshold criteria near these values were experimented with and gave similar results (results did not appear to be dependent on threshold criteria).

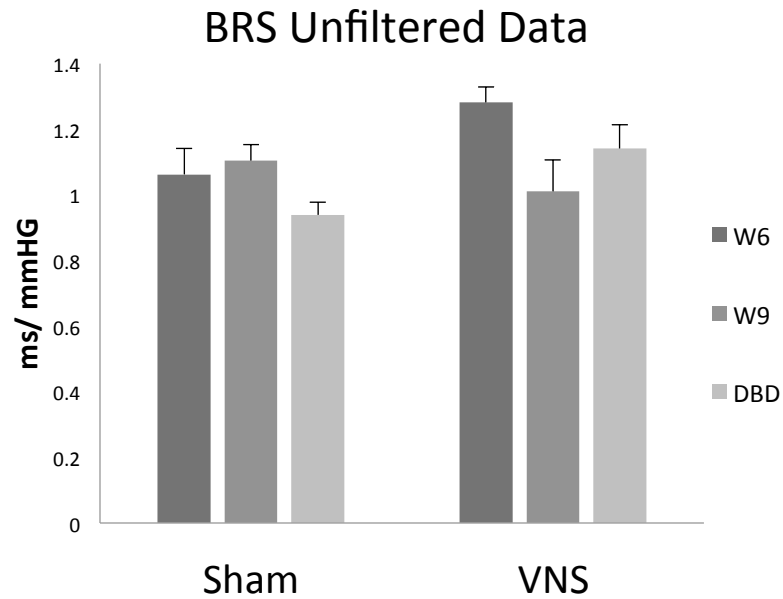


Figure 3.9: Baroreflex Sensitivity (BRS) unfiltered data: Minimum Sequence Count = 4, Minimum Required Increase/Decrease in Pressure = 1 mmHG, Minimum $R^2 = 0.9$

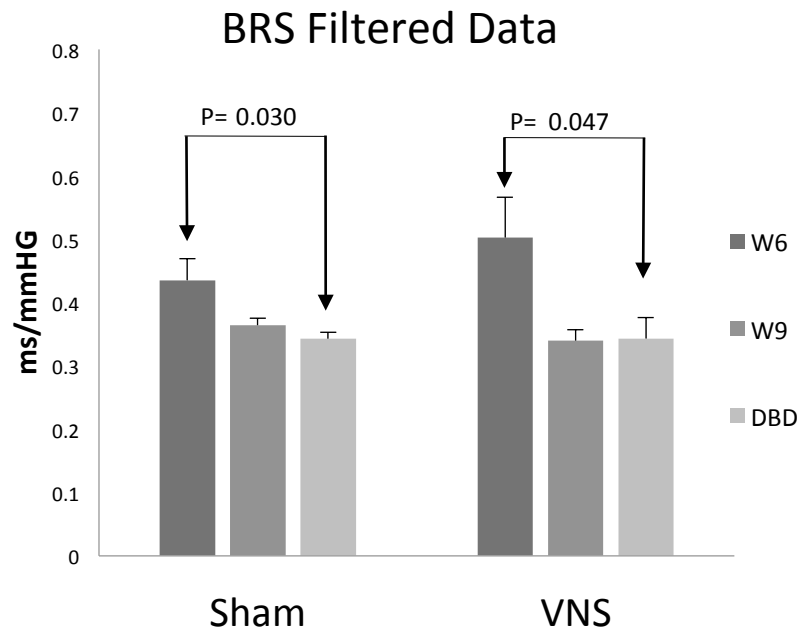


Figure 3.10: Baroreflex Sensitivity (BRS), low pass filtered data to remove breathing frequency. Minimum Sequence Count = 16, Minimum Required Increase/Decrease in Pressure = 5 mmHg, Minimum $R^2 = 0.9$

CHAPTER 4: DISCUSSION

Survival Data

Survival data shows that VNS rats outlived Sham rats ($P < 0.05$). This implies that VNS was able to significantly alter the physiology of the rats.

Average BP and HR

Both Sham and VNS rats experienced statistically significant increases in mean SBP during the period from 10PM – 2AM. It is somewhat surprising that an attenuation of BP did not occur in VNS relative to Sham. One possible explanation relates to data from a previous study in our lab demonstrating that VNS induces greater modulation of MAP during the daytime, when the nocturnal rats are less active [20]. Data in our current study was collected at night, when rats are awake and sympathetic activity dominates. During this time, VNS may be less able to produce an attenuation in BP. A second explanation is that VNS may exert therapeutic effects independently of BP changes, or that BP changes take longer to occur than other therapeutic effects. Zhang et al. showed that in dogs, therapeutic effects of VNS resulted without any change in systemic BP [23]. Thus, similarities in BP for Sham and VNS rats are due in part to day/night activity, but in addition, VNS might produce certain therapeutic effects more immediately by down-regulating the SNS, but large changes in BP can take longer to achieve.

There were no statistically significant differences in mean HR from W6 to DBD for either group, although VNS rats did display a slight decrease in HR, which may reflect the acute bradycardic effect of VNS. A significant acute bradycardic effect was observed in only 1 of the VNS rats.

Although analysis of survival data implies that physiological changes are occurring as a result of VNS, no firm conclusions can be drawn based solely on the mean HR and BP data presented here. This fact emphasizes the need for additional analytic techniques to elucidate underlying physiology, which was a primary motivating factor for this thesis research.

Frequency Domain Parameters – Unresolved Questions

It is recommended that Appendix A be read before the following sections. As discussed there, the use of frequency domain analysis and specifically the use of HF power, LF power, and the LF/HF ratio as parameters to gauge autonomic balance is an appealing research technique. However, several questions remain regarding the application of spectral analysis to this data. Firstly, physiological correlates of LF power remain controversial, and the use of the LF band as a marker of autonomic tone is questionable (see Appendix A) [40]. Secondly, if one were to use LF power as a marker of autonomic balance, it would seem necessary to witness a “peak” in the LF power spectrum range, or at least observe distinct LF oscillations in the HR and BP trace. For data here, no peak was found in the LF range, and no consistent “Mayer Waves” were seen. It remains unclear whether the observation of an LF peak is necessary to conduct

spectral analysis. It may be that in order to observe the LF peak, spectral analysis must be conducted under laboratory conditions in which physical activity and breathing are controlled. Parati cites this as a necessary condition for short-term spectral analysis but it appears many authors do not adhere to this requirement [41]. Lastly, there seems to be disagreement on what range constitutes the low frequency band in rats. As seen in Table 2.1, authors use different values, so it is unclear which range is correct. It would seem logical that the band should be based on the data, and centered on the LF peak, but again, no LF peak was observed.

In conclusion, there are too many questions surrounding the use of LF power as an analysis tool to warrant its use in this study. In contrast, most authors agree on the correlation between high frequency oscillations in HR and level of parasympathetic cardiac control; therefore, HF and RMSSD are included in our analysis. HF band ranges vary between studies in rats, but are usually between 0.75 – 5 Hz, covering the respiratory frequency in rats of about 85 breaths/min (1.4 Hz), which can be elevated in cardiovascular disease. An HF respiratory peak was present for rats in this study (see Figure 2.11). Lastly, VLF power was not used because values for this range are not fully established in rats, and ULF power was not measured because the data segments were too short to pick up these low frequencies.

Effects of Hypertension on Sham Rats

High Frequency Oscillations in Sham Rats

RMSSD and HF power for HRV, which aim to quantify oscillations due to respiration, decrease significantly in Sham rats from W6 to DBD ($P = 0.021$, $P = 0.032$, respectively). BRS of “unfiltered” data follows a similar trend in Sham rats (although without statistical significance), decreasing from W6 to DBD (Figure 3.9). Lastly, RMSSD and HF power of BP increase during the same time period, which may indicate that these BP oscillations are not being effectively buffered. In summary, in hypertension, respiratory sinus arrhythmia decreased along with BRS at the respiratory frequency, and BP oscillations due to respiration increased.

While many interpret reduced respiratory sinus arrhythmia to reflect a reduced parasympathetic cardiac control, a cautious analysis should be used here. Both high frequency HRV and high frequency BRS decrease, and there likely is a cause/effect relationship between the two variables. Specifically, it appears that HR and BP are becoming “uncoupled” due to the progression of HTN at the respiratory rate and this uncoupling is caused by a dysfunction in the baroreflex. This dysfunction may occur anywhere along the baroreflex arc (Figure 4.1), and does not necessarily indicate that the problem lies in the efferent parasympathetic innervation of the heart (vagal tone). Other possibilities could include alterations in the baroreceptors themselves or changes in brain processing centers [42].

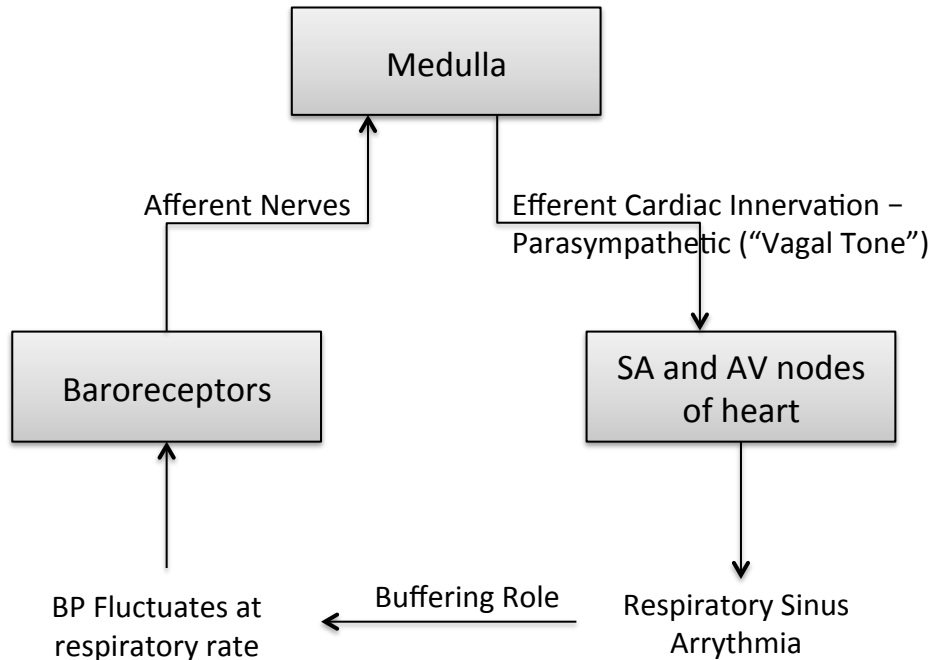


Figure 4.1: Simplified baroreflex arc involved in respiratory sinus arrhythmia. Loss of RSA could occur through different means.

Lower Frequency Oscillations and Overall HRV and BPV in Sham Rats

Decreases in lower frequency oscillations and overall HRV and BPV are seen without statistical significance in the Sham group from W6 to DBD in SDNN ($P = 0.09$) and SDANN ($P=0.23$). SDNN reflects total HRV while SDANN reflects HRV with periods over 5 minutes and corresponds to variability from slower hormonal processes. The decreases in these variables likely reflect the negative physiological effects of HTN, although it is difficult to trace these parameters back to an exact physiological mechanism. A reduction in overall HRV may reflect a decrease in vagal activity leading to a prevalence of sympathetic mechanisms and cardiac electrical instability [17]. Henze et al showed that SDANN and SDNN were reduced early on in a rat model of heart

failure, owing to a progressive loss of baroreflex modulation of sympathetic tone [29].

Therefore, the increase in SDNN and SDANN in Sham rats seen here provides tentative evidence of the well-known overactive SNS in HTN. More convincingly, it confirms the prognostic value associated with these metrics and with overall HRV; qualitatively, the reduced HRV in Sham rats is consistent with the survival data trends.

ASDNN results are less ambivalent with Sham rats decreasing from W6 to DBD ($P = 0.01$). ASDNN essentially removes oscillations with periods longer than 5 minutes. As mentioned, oscillations with periods over 5 minutes are not well understood, but are likely mediated by longer-term humoral control mechanisms, or by circadian rhythms [13]. With these oscillations removed, ASDNN may be more reflective of the faster responding systems including any baroreflex-mediated oscillations, and those involving autonomic innervation. Decreases in ASDNN may indicate increased sympathetic activity over parasympathetic activity.

VNS Rats: Effects of Stimulation

High Frequency Oscillations in VNS rats

No statistical significance was found in parameters that gauge high frequency fluctuations due to respiration in VNS rats, making analysis in this section somewhat speculative. Qualitatively, it appears that HTN exerts negative physiological effects from W6 to W9 in VNS rats. Similar trends to Sham rats are seen: RMSSD and HF power in HR decrease, BRS at the respiratory frequency decreases, and RMSSD and HF power in BP increase. However, from W9 to DBD, all of these trends reverse. This may indicate

that VNS is able to preserve or remedy the coupling between HR and BP at the respiratory frequency. Data from a larger number of rats is needed to validate these claims.

Lower Frequency Oscillations and Overall HRV and BPV in VNS Rats

The significant decreases in overall HRV that are seen in Sham rats are not present in VNS rats. SDNN and SDANN qualitatively appear to increase from W9 to DBD. As mentioned, this HRV data is able to corroborate survival data: it appears that the higher survival rate in VNS corresponds to increased HRV at lower frequencies as depicted by SDNN and SDANN. BPV data in VNS rats is largely inconclusive except for ASDNN, which increases from W6 to DBD ($P = 0.012$). As discussed, ASDNN represents oscillations with periods under 5 minutes. With respect to VNS, the marked increase in ASDNN in BPV may be due to a loss of baroreflex control. BRS of filtered data shows that baroreflex control at frequencies below respiration is lost in both Sham and VNS rats ($P = 0.030$ and $P = 0.047$ respectively), as discussed in the next section.

Baroreflex Sensitivity

The threshold criteria listed in Figure 3.6 (minimum sequence count of 4, minimum required change in pressure of 1 mmHg and minimum R^2 of 0.9) are in line with other published studies that have described or used the sequence method [29], [36], [38], [39], [43]. Unfortunately, a limited number of studies exist on the sequence method's use in rats. Henze et al found BRS values of normal Sprague-Dawley rats to fall within the

ranges of 1-3 ms/mmHg and that in rats with chronic heart failure BRS significantly decreased [29]. Stauss found BRS in rats calculated from the sequence method to lie between 0.5 ms/mmHg and 1.5 ms/mmHg [43]. Thus, BRS results on unfiltered data in this study are in agreement with other studies conducted on rats.

We are aware of no other study that uses low pass filtering prior to application of the sequence algorithm; however, when considering the goal of the sequence method – to quantify changes in PI that result from changes in BP – this technique seems valid. Additionally, there have been efforts at quantifying the baroreflex using spectral methods that aim to divide coherence in BP and HR into different frequency bands [37], [38]; filtering the data prior to the sequence technique can be seen as a time domain correlate to these spectral methods. In addition, most of the sequences captured by this technique are similar to those pictured in Figure 2.15; visually, it appears the baroreflex is operating, providing further justification for the use of filtering in conjunction with the sequence method.

As discussed, BRS results provide evidence that the efficacy of the baroreflex at the breathing frequency is reduced from W6 to DBD in Sham rats and not in VNS rats. BRS of filtered data reflects BP and HR interactions at frequencies below respiration. For both Sham and VNS rats, BRS of filtered data decreases from W6 to DBD ($P = 0.030$, $P = 0.047$, respectively). Impaired BRS could be the result of abnormalities seen anywhere along the baroreflex arc [44]. Impaired BRS has been associated with HTN, increased sympathetic tone, and increased arterial stiffness [6], [45]. One proposed mechanism of

reduced BRS in HTN is that a reduced vascular compliance in the baroreceptor areas causes reduced afferent firing (stretch of the vessels is limited due to stiffening); The brain interprets this reduced afferent firing as lower BP, and therefore stimulates SNS action which predominates over PNS activity [6], [7]. Regardless of the exact mechanisms of reduced BRS, there is little question regarding its association with HTN. Reduced BRS is seen in almost all hypertensive patients, and as HTN progresses, BRS decreases [46].

Limitations

Decisions we made early on in the project led to some difficulties for later analysis. The time used for analysis was chosen at the beginning of the study as 10PM-2AM. Two problems arise from this choice. First, the use of nighttime data may diminish physiological manifestations of VNS [20]. Therefore it is advisable to use daytime data in order to better distinguish differences between VNS and Sham. Second, SDNN, SDANN and ASDNN are usually calculated over 24 hours, so the fact that this data was taken over shorter time periods may have produced less substantial results. Specifically, if SDNN and SDANN were calculated over 24 hours for Sham rats, it is likely that even more pronounced differences between W6 and DBD would be observed, since HTN tends to diminish HR changes due to circadian rhythm.

In some rats, atrial fibrillation (AF) was present. This does not lead to problems in PI detection, but AF episodes often caused significant decreases in pressure and sometimes corresponding increases in HR. These episodes are not “filterable” like other

arrhythmias. It is uncertain what affect these AF episodes had on BPV and HRV results. Additionally, VNS caused acute changes in BP and HR under rare circumstances. By changing HR and BP, VNS could lead to “artificial” HRV and BPV. These effects are likely minimal in our study since acute effects of VNS were only seen in 1 VNS rat.

Future Work and Recommendations

A future study should analyze 24-hour variability, since HTN is thought to be significantly affected by circadian rhythms. Additionally, shorter data segments should be collected and analyzed in the daytime from 10AM-2PM, since VNS may have more marked effects when rats are sleeping. If problems surrounding frequency domain analysis are sufficiently solved, an analysis of LF power and the LF/HF ratio may be undertaken to provide further insight into the autonomic balance in VNS and hypertensive rats.

Additionally, frequency domain methods can be used to validate results obtained here using the sequence method. Baroreflex sensitivity algorithms in the frequency domain compute a spectral BP to PI transfer function, which can be computed over specific frequencies. Therefore, this technique can be used to validate the sequence method applied to unfiltered data and filtered data.

CHAPTER 5: CONCLUSION

We set out to explore and identify various metrics that can be extracted from ECG and pressure data for use in evaluating physiological effects of HTN, and of VNS-treated HTN. HRV, BPV, and BRS emerged as promising parameters that can provide a wealth of physiological and pathological information. In order to calculate these parameters, we discovered that considerable thought and effort must be placed in the “pre-processing” of data; that is, how to acquire a clean data set free from noise and ectopic beats. We developed methods to conduct effective pre-processing; first, using ECG and pressure data, and then, due to fickle ECG traces, using solely pressure data. We developed a QRS detection algorithm using pressure and ECG data that could reliably detect the QRS peak during VNS “on” periods. Then, using pressure data alone, we developed a novel technique to calculate pulse interval from the derivative of the pressure trace, which proved to be more accurate than calculating pulse interval from the pressure trace alone.

We primarily used time domain parameters in this study to evaluate HRV and BPV. We created frequency domain techniques in MATLAB to analyze HRV and BPV, but too many questions arose surrounding these parameters to warrant their widespread use in this study; in subsequent work, these questions may be answered and frequency methods may be more reliably used. In addition, BRS quantification was conducted in the time domain using the sequence method.

Our results confirm HRV, BPV, and BRS parameters can be used successfully to quantify pathophysiology in hypertension and that VNS leads to therapeutic physiological effects. We draw several conclusions as to the physiological effects of HTN and VNS. First, HTN leads to an uncoupling of BP and HR at the respiratory rate, and this uncoupling is prevented in VNS rats. This may indicate that VNS is preserving vagal tone, although our study cannot confirm an exact mechanism. Overall and lower frequency HRV appears to be partially retained in VNS rats compared with Sham rats. To further evaluate the effects of VNS, studies of larger numbers of rats during the sleep cycle (day time) should be completed, as well as a 24-hour data analysis to elucidate HTN and VNS effects on circadian rhythms.

REFERENCES

- [1] R. E. Klabunde, *Cardiovascular Physiology Concepts*. Lippincott Williams & Wilkins, 2012.
- [2] R. Meraï *et al.*, “CDC Grand Rounds: A Public Health Approach to Detect and Control Hypertension,” *MMWR. Morb. Mortal. Wkly. Rep.*, vol. 65, no. 45, pp. 1261–1264, Nov. 2016.
- [3] G. Mancia *et al.*, “2007 Guidelines for the Management of Arterial Hypertension,” *J. Hypertens.*, vol. 25, no. 6, pp. 1105–1187, Jun. 2007.
- [4] J. P. Fisher and J. F. R. Paton, “The sympathetic nervous system and blood pressure in humans: implications for hypertension,” *J. Hum. Hypertens.*, vol. 26, no. 8, pp. 463–75, 2012.
- [5] D. A. Calhoun *et al.*, “Resistant hypertension: diagnosis, evaluation, and treatment: a scientific statement from the American Heart Association Professional Education Committee of the Council for High Blood Pressure Research,” *Circulation*, vol. 117, no. 25, pp. e510–e526, Jun. 2008.
- [6] E. R. Carthy, “Autonomic dysfunction in essential hypertension: A systematic review,” *Ann. Med. Surg.*, vol. 3, no. 1, pp. 2–7, 2014.
- [7] G. Mancia and G. Grassi, “The autonomic nervous system and hypertension,” *Circ. Res.*, vol. 114, no. 11, pp. 1804–1814, 2014.
- [8] M. Pagani and D. Lucini, “Autonomic dysregulation in essential hypertension: Insight from heart rate and arterial pressure variability,” *Auton. Neurosci. Basic Clin.*, vol. 90, no. 1–2, pp. 76–82, 2001.
- [9] L. Clademenos, “Blood Pressure,” *Sharinginhealth*, 2012. [Online]. Available: http://www.sharinginhealth.ca/biology/blood_pressure.html. [Accessed: 29-Mar-2017].
- [10] G. G. Berntson *et al.*, “Heart rate variability: origins, methods, and interpretive caveats,” *Psychophysiology*, vol. 34, no. 6, pp. 623–48, 1997.
- [11] H. M. Stauss, P. B. Persson, A. K. Johnson, and K. C. Kregel, “Frequency-response characteristics of autonomic nervous system function in conscious rats,” *Am. J. Physiol.*, vol. 273, no. 2 Pt 2, pp. H786–95, Aug. 1997.
- [12] H. M. Stauss, “Physiologic Mechanisms of Heart Rate Variability,” vol. 14, no. 1, pp. 8–15, 2006.
- [13] H. M. Stauss, “Identification of blood pressure control mechanisms by power spectral analysis,” *Clin. Exp. Pharmacol. Physiol.*, vol. 34, no. 4, pp. 362–368, 2007.
- [14] G. E. Billman, “Heart rate variability - A historical perspective,” *Front. Physiol.*, vol. 2 NOV, p. 86, 2011.
- [15] G. E. Billman, H. Kuikuri, J. Sacah, and K. Trimmel, *An introduction to heart rate variability : methodological considerations and clinical applications*, vol. 6, no. February. Frontiers Media SA, 2015, pp. 2013–2015.

- [16] “Heart rate Variability: new perspectives on physiological Mechanisms, assessment of self-regulatory Capacity, and Health risk,” vol. 46, no. 1, 2015.
- [17] “Heart rate variability: standards of measurement, physiological interpretation and clinical use. Task Force of the European Society of Cardiology and the North American Society of Pacing and Electrophysiology,” *Circulation*, vol. 93, no. 5, pp. 1043–65, Mar. 1996.
- [18] G. Parati, G. Mancia, M. Di Rienzo, P. Castiglioni, A. Taylor, and P. Studinger, “Point : Counterpoint Point : Counterpoint : Cardiovascular variability is / is not an index of autonomic control of circulation,” *J. Appl. Physiol.*, vol. 101, no. 2, pp. 676–682, 2006.
- [19] E. B. Schroeder, D. Liao, L. E. Chambless, R. J. Prineas, G. W. Evans, and G. Heiss, “Hypertension, Blood Pressure, and Heart Rate Variability: The Atherosclerosis Risk in Communities (ARIC) Study,” *Hypertension*, vol. 42, no. 6, pp. 1106–1111, 2003.
- [20] E. M. Annoni *et al.*, “Intermittent electrical stimulation of the right cervical vagus nerve in salt-sensitive hypertensive rats: effects on blood pressure, arrhythmias, and ventricular electrophysiology,” *Physiol. Rep.*, vol. 3, no. 8, p. e12476, 2015.
- [21] R. E. Kleiger, P. K. Stein, and J. T. Bigger, “Heart rate variability: Measurement and clinical utility,” *Ann. Noninvasive Electrocardiol.*, vol. 10, no. 1, pp. 88–101, 2005.
- [22] S. Bibevski and M. E. Dunlap, “Prevention of diminished parasympathetic control of the heart in experimental heart failure,” *Am. J. Physiol. Heart Circ. Physiol.*, vol. 287, no. 4, pp. H1780-5, 2004.
- [23] Y. Zhang *et al.*, “Chronic vagus nerve stimulation improves autonomic control and attenuates systemic inflammation and heart failure progression in a canine high-rate pacing model,” *Circ. Hear. Fail.*, vol. 2, no. 6, pp. 692–699, 2009.
- [24] Y. Kakinuma *et al.*, “Acetylcholine from vagal stimulation protects cardiomyocytes against ischemia and hypoxia involving additive non-hypoxic induction of HIF-1??,” *FEBS Lett.*, vol. 579, no. 10, pp. 2111–2118, 2005.
- [25] M. N. Levy and B. Blattberg, “Effect of vagal stimulation on the overflow of norepinephrine into the coronary sinus during cardiac sympathetic nerve stimulation in the dog,” *Circ. Res.*, vol. 38, no. 2, pp. 81–84, 1976.
- [26] G. Mancia, J. C. Romero, and J. T. Shepherd, “Continuous inhibition of renin release in dogs by vagally innervated receptors in the cardiopulmonary region,” *Circ. Res.*, vol. 36, no. 4, pp. 529–535, 1975.
- [27] B. L. K. Dahl, K. D. Knudsen, M. A. Heine, and G. J. Leitl, “Effects of Chronic Excess Salt Ingestion: Modification of Experimental Hypertension in the Rat by Variations in Diet,” pp. 11–19.
- [28] M. A. Peltola, “Role of editing of R-R intervals in the analysis of heart rate variability,” *Front. Physiol.*, vol. 3 MAY, no. May, pp. 1–10, 2012.
- [29] M. Henze, D. Hart, A. Samarel, J. Barakat, L. Eckert, and K. Scrogin, “Persistent alterations in heart rate variability, baroreflex sensitivity, and anxiety-like

- behaviors during development of heart failure in the rat.," *Am. J. Physiol. Heart Circ. Physiol.*, vol. 295, no. 1, pp. H29–H38, 2008.
- [30] C. Cerutti, C. Barres, and C. Paultre, "Baroreflex modulation of blood pressure and heart rate variabilities in rats: assessment by spectral analysis.," *Am. J. Physiol.*, vol. 266, no. 5 Pt 2, pp. H1993–H2000, 1994.
 - [31] C. Cerutti *et al.*, "Autonomic nervous system and cardiovascular variability in rats: a spectral analysis approach.," *Am. J. Physiol.*, vol. 261, no. 4 Pt 2, pp. H1292–9, 1991.
 - [32] E. Aubert *et al.*, "The analysis of heart rate variability in unrestrained rats . Validation of method and results," *Comput. Methods Programs Biomed.*, vol. 60, pp. 197–213, 1999.
 - [33] G. Ning, Y. Bai, W. Yan, and X. Zheng, "Investigation of beat-to-beat cardiovascular activity of rats by radio telemetry.," *Clin. Hemorheol. Microcirc.*, vol. 34, no. 1–2, pp. 363–71, 2006.
 - [34] H. Sedghamiz, "Complete Pan Tompkins Implementation ECG QRS detector - File Exchange - MATLAB Central," *Complete Pan Tompkins Implementation ECG QRS detector*. [Online]. Available: <https://www.mathworks.com/matlabcentral/fileexchange/45840-complete-pan-tompkins-implementation-ecg-qrs-detector>. [Accessed: 06-May-2017].
 - [35] E. Ades, "Species Specific Information: Rat," *Johns Hopkins Univ.*, pp. 1–9, 2015.
 - [36] G. Bertinieri, M. Di Rienzo, A. Cavallazzi, A. Ferrari, A. Pedotti, and G. Mancia, "A New Approach to Analysis of the Arterial Baroreflex," *J. Hypertens.*, 1985.
 - [37] C. A. Swenne, "Baroreflex sensitivity: Mechanisms and measurement," *Netherlands Hear. J.*, vol. 21, no. 2, pp. 58–60, 2013.
 - [38] G. Parati, M. Di Rienzo, and G. Mancia, "How to measure baroreflex sensitivity: from the cardiovascular laboratory to daily life.," *J. Hypertens.*, vol. 18, no. 1, pp. 7–19, 2000.
 - [39] D. Laude *et al.*, "Comparison of various techniques used to estimate spontaneous baroreflex sensitivity (the EuroBaVar study).," *Am. J. Physiol. Regul. Integr. Comp. Physiol.*, vol. 286, no. 1, pp. R226–R231, 2004.
 - [40] G. E. Billman, "The LF/HF ratio does not accurately measure cardiac sympatho-vagal balance," *Front. Physiol.*, vol. 4 FEB, no. February, pp. 1–5, 2013.
 - [41] G. Parati, J. P. Saul, M. Di Rienzo, and G. Mancia, "Spectral Analysis of Blood Pressure and Heart Rate Variability in Evaluating Cardiovascular Regulation: A Critical Appraisal," *Hypertension*, vol. 25, no. 6, pp. 1276–1286, Jun. 1995.
 - [42] V. E. Papaioannou, "Heart rate variability, baroreflex function and heart rate turbulence: possible origin and implications.," *Hellenic J. Cardiol.*, vol. 48, no. 5, pp. 278–89, 2007.
 - [43] H. M. Stauss, "Baroreceptor Reflex Sensitivity Estimated by the Sequence Technique is Reliable in Rats," *Amerian J. Physiol. Hear. Circ. Physiol.*, vol. 288, pp. 2422–2430, 2005.
 - [44] F. J. Gordon and A. L. Mark, "Mechanism of impaired baroreflex control in

- prehypertensive Dahl salt-sensitive rats,” *Circ. Res.*, vol. 54, no. 4, pp. 378–387, Apr. 1984.
- [45] F. U. S. Mattace-Raso *et al.*, “Arterial stiffness, cardiovagal baroreflex sensitivity and postural blood pressure changes in older adults: the Rotterdam Study,” *J. Hypertens.*, vol. 25, no. 7, pp. 1421–1426, 2007.
 - [46] B. Gribbin, T. G. Pickering, P. Sleight, and R. Peto, “Effect of age and high blood pressure on baroreflex sensitivity in man,” *Circ. Res.*, vol. 29, pp. 424–431, 1971.
 - [47] M. Di Rienzo, G. Parati, A. Radaelli, and P. Castiglioni, “Baroreflex contribution to blood pressure and heart rate oscillations: time scales, time-variant characteristics and nonlinearities,” *Philos. Trans. A. Math. Phys. Eng. Sci.*, vol. 367, no. 1892, pp. 1301–1318, Apr. 2009.
 - [48] S. C. Malpas, “Invited review,” *Muscle Nerve*, no. March, pp. 339–351, 2004.
 - [49] F. Yasuma and J. I. Hayano, “Respiratory Sinus Arrhythmia: Why Does the Heartbeat Synchronize with Respiratory Rhythm?,” *Chest*, vol. 125, no. 2, pp. 683–690, Feb-2004.
 - [50] R. W. De Boer, J. M. Karemaker, and J. Strackee, “Hemodynamic fluctuations and baroreflex sensitivity in humans: a beat-to-beat model,” *Am. J. Physiol.*, vol. 253, no. 3, pp. H680–H689, 1987.
 - [51] L. Bernardi *et al.*, “Respiratory sinus arrhythmia in the denervated human heart,” *J. Appl. Physiol.*, vol. 67, no. 4, pp. 1447–55, 1989.
 - [52] A. Malliani, M. Pagani, F. Lombardi, and S. Cerutti, “Cardiovascular neural regulation explored in the frequency domain,” *Circulation*, vol. 84, no. 2, pp. 482–492, 1991.
 - [53] A. E. Draghici and J. A. Taylor, “The Physiological Basis and Measurement of Heart Rate Variability in Humans,” *J. Physiol. Anthropol.*, vol. 35, no. 1, pp. 22–29, 2016.
 - [54] P. Lanfranchi and V. Somers, “Arterial Baroreflex Function and Cardiovascular Variability: Interactions and Implications,” *Am. J. Physiol. Regul. Integr. Comp. Physiol.*, no. March, pp. 339–351, 2004.
 - [55] C. Julien, “The enigma of Mayer waves: Facts and models,” *Cardiovasc. Res.*, vol. 70, no. 1, pp. 12–21, 2006.
 - [56] S. Guzzetti *et al.*, “Sympathetic predominance in essential hypertension: a study employing spectral analysis of heart rate variability,” *Journal of hypertension*, vol. 6, no. 9, pp. 711–7, 1988.

APPENDIX A: PHYSIOLOGICAL CORRELATES OF CARDIOVASCULAR OSCILLATIONS

HR is often thought of as a modulator of BP, through several different control mechanisms. If the circuitry of these controls mechanisms malfunctions, an inability of the body to respond to perturbations in BP is seen as an increased BPV and a decreased HRV. Therefore on simplistic level, decreases in overall HRV over time are seen as unhealthy, and increases in overall BPV over time are seen as unhealthy, although an examination of variability at certain frequencies can reveal deeper insights into physiology.

“High Frequency (HF)” Oscillations:

It is generally accepted that HF oscillations in both BP and HR occur primarily as a result of respiration [17], [18], [47]. These HF oscillations in HR are often referred to as respiratory sinus arrhythmia (RSA). The mechanical hypothesis of RSA states that the act of respiration mechanically induces fluctuations in venous return, CO, and thus BP [47]–[50]. Proof that BP changes at this frequency are mechanically mediated come from experiments that show that when the baroreflex is deactivated, such as in brain-dead patients, HF BP oscillations induced by the mechanical ventilator are still present [47]. In addition, HF BP oscillations remain active in denervated donor hearts [51].

These fluctuations in BP are then thought to activate the baroreflex to induce corresponding oscillations in HR. Through the baroreceptor reflex, efferent nerves responding to respiratory oscillations in BP are able to innervate the heart to produce corresponding fluctuations in HR. Efferent innervation of the heart at this high frequency occurs almost exclusively through vagal input, since the SNS is not fast enough to respond [12], [47]. Therefore metrics that aim to measure the amplitude of HF HR oscillations, such as RMSSD, and HF power, are often used as indicators of vagal tone [18], [48]. Support for these indicators come from studies in which atropine administration (a parasympathetic blocker) abolishes almost all oscillations in HR at the respiratory frequency, while HF oscillations of BP remain intact [31], [52]. De Boer et al created a beat-to-beat mathematical model of HRV which supports the theory that respiratory oscillations in HR are secondary to BP oscillations [50]. Pictorial representation of the model is displayed in Figure A1. While a majority of the literature investigated in this study supported the use of HRV at respiratory frequencies as indicative of “vagal tone,” some authors expressed skepticism [48], [53]. The fact that some HR oscillations remain after combined cardiac sympathetic and vagal blockade indicates that in addition to the vagally-mediated baroreflex pathway, there are other non-autonomic HF regulators of HR, such as intra-cardiac reflexes and mechanical stretching of the SA node [10], [54]. Additionally, a reduced HRV at the respiratory frequency may reflect changes in other variables along the baroreflex arc. For example, “vagal tone” may be adequate, but if the afferent nerves or baroreceptors themselves become less

responsive, this may lead to a decrease in HF HR oscillations. In summary, high frequency HRV is an adequate measure of vagal cardiac control, but should be analyzed with caution, and if possible in the context of other HRV and BPV data.

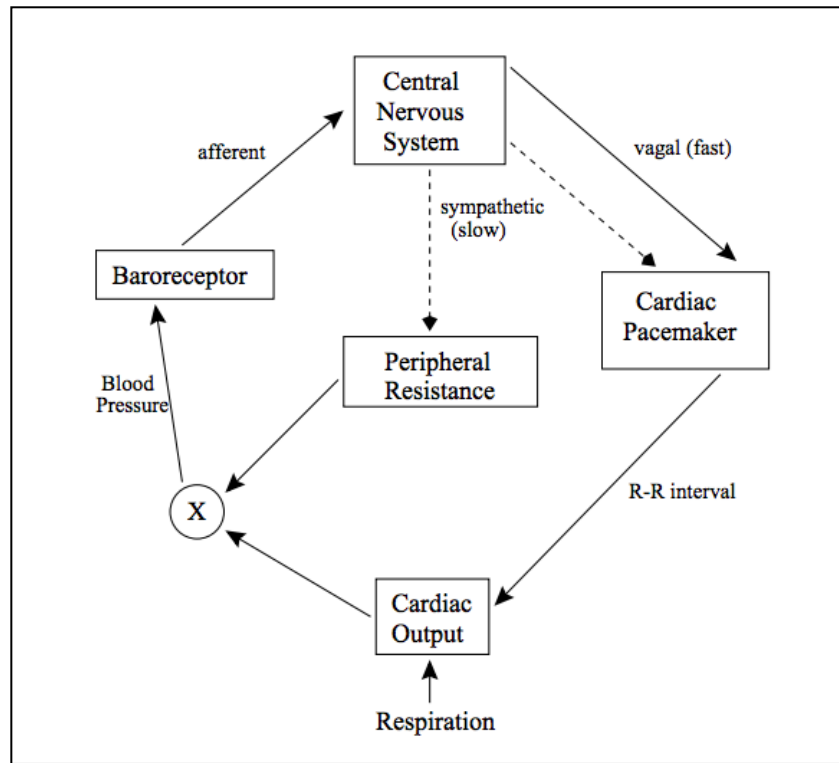


Figure A1: DeBoer's Model BP Control. Note how RSA is mediated through the "fast" vagal efferent nerves.

"Low Frequency (LF)" Oscillations

Mechanisms of LF oscillations in HR and BP are less understood and their representation of the ANS more controversial. The so-called "Mayer waves" are seen at 0.1 Hz in humans and 0.4 Hz in rats [13], [48]. They have been used as a marker of sympathetic activity despite an unclear understanding of their underlying physiology.

There are two prevailing theories for these LF oscillations: the central oscillator theory and the baroreflex feedback loop theory. The central oscillatory theory states that LF oscillations are generated by brain stem circuits independent of any sensory input [42], [48], [55]. These brain stem circuits generate oscillations in efferent sympathetic nervous activity (SNA) which results in a oscillations in vasomotor tone, and therefore BP. Corresponding oscillations in HR then appear through the baroreflex and are thought to buffer, rather than enhance the BP oscillations. In contrast, the baroreflex feedback loop theory, postulates that LF oscillations in both BP and HR are ultimately due to respiration. The baroreceptors sense the respiratory-induced changes in BP; the fast vagal response causes RSA, but there is also a slower sympathetic response. This slower sympathetic response's interaction with the faster vagal response initiates changes in HR and BP at lower frequencies. There are slight variations of this theory involving various resonance feedback loops involved in the baroreflex arc.

Regardless of the theory, historically, LF oscillations have often been used as a marker of sympathetic tone and the LF/HF ratio as a marker of autonomic balance; however, many have reported the dubious nature of this index [16], [41], [48]. Instead, these fluctuations have been shown to have both sympathetic and parasympathetic origins; both parasympathetic blockade with atropine and sympathetic blockade with propranolol reduce HR oscillations in the LF band [21], [41]. In summary, the LF band in HRV mainly represents fluctuations in sympathetic and vagal input to the heart that result from variations in BP, however, non-autonomic influences may also play a role.

The LF band in BPV seems to be more accepted as a measure of exclusively sympathetic tone, but questions still remain on its use.

“Very Low Frequency (VLF)” Oscillations

The physiological basis for VLF oscillations is still under investigation, although VLF measures have the most significant prognostic value in humans. Decreases in this band over time have stronger associations to all-cause mortality than either the LF or HF bands [16]. Mechanisms involved in VLF fluctuations are thought to be related to ANS interactions with thermoregulation, the RAAS, vasomotor activity and other hormonal factors. Efferent sympathetic activity has been shown to modulate some of these oscillations; and increases in VLF power or shifting of their frequency may reflect increases in efferent sympathetic activity [16]. However, VLF oscillations in HR are abolished by atropine, indicating that the PNS plays a role as well [21]. ACE inhibition also reduces VLF power by approximately 20%, indicating that the RAAS system also plays a role [21]. In this study, VLF oscillations contribute significantly to the time domain metrics SDNN, SDANN, and ASDNN.

“Ultra-Low Frequency ULF” oscillations

This band represents fluctuations with periods over 5 minutes. Like the VLF band, the physiological causes of oscillations in the ULF band is still under investigation. The ULF band is able to capture day-night differences, so circadian rhythms play a

dominant role, but other slow moving hormonal systems such as the RAAS may also contribute [16]. This study is not able to measure the ULF band accurately since the data segments are too short.

Frequency Domain Analysis and Hypertension

In HTN, an overactive SNS or underactive PNS can manifest in HRV and BPV in several ways. Guzzetti et al reported that patients with essential HTN are characterized by a greater LF power and a smaller HF power of RR interval compared with normotensives [56]. These results were interpreted as symptomatic of reduced vagal tone and increased SNS activity. The LF band in BPV is enhanced in hypertensives, which may represent enhanced peripheral sympathetic drive [8]. At frequencies below the LF band, HTN is reported to cause decreases in HRV and increases BPV; the mechanisms of these changes are not as well known, although hormonal systems with overactive sympathetic inputs, such as the RAAS, may play significant roles [41].

APPENDIX B: INSTRUCTIONS FOR MATLAB

This thesis is accompanied by MATLAB code. Brief instructions are presented here but code is also commented with explanations.

Place all analysis files and MATLAB functions into same folder. Update LoadData.m to reflect ASCII file names. Run LoadData.m. This will create variables ECGLoad.m, PressureLoad.m, and tLoad.m and saves them to the workspace. Next, run RemoveSaturation.m. This removes all saturated segments from pressure signals (and ECG) and creates variables ECGcut, PressureCut, and tCut. This script calculates the shortest data segment and normalizes all segments to this length. For data analyzed here, minimum length was 168 minutes.

Next, run CleanAllData.m. This file calculates SBPs and calculates pulse interval from the derivative of the pressure trace. It also matches SBP and subsequent PI with a delay of 1 (this delay can be adjusted). It also removes arrhythmic artifacts from SBP and PI data by calling the function “InterpolateArrhythmias.” This function produces a cell, called “CleanDataCell.m,” which contains PI data set and corresponding time, and SBP data set and corresponding time.

Once the variable CleanDataCell.m is acquired with data, “post-processing” analysis functions/scripts can operate on the data stored within it. The three main scripts for analysis are: BPVandHRV.m, FrequencyMethods.m, and Script_For_Sequence_Method.m. Use BPVandHRV.m to calculate time domain HRV

and BPV parameters: SDNN, RMMSD, SDANN, ASSDNN. Use FrequencyMethods.m to calculate frequency domain parameters: HF, LF, VLF, ULF, and total power. Use Script_For_Sequence_Method.m, which calls “SequenceMethodFunction.m” to calculate BRS and other parameters associated with the sequence method.